AN EXPERIMENTAL INVESTIGATION OF THE INCIPIENT DRAWDOWN CONDITIONS IN TWO-LAYERED STRATIFIED FLOW

AN EXPERIMENTAL INVESTIGATION OF THE INCIPIENT DRAWDOWN CONDITIONS IN TWO-LAYERED STRATIFIED FLOW

BY

SUBHASH GUPTA

A Thesis

Submitted to the Faculty of Graduate Studies

in Partial Fulfilment of the Requirements

for the Degree

Master of Engineering

McMaster University

February, 1969

MASTER OF ENGINEERING
Mechanical Engineering

McMASTER UNIVERSITY
Hamilton, Ontario

TITLE: An Experimental Investigation of the Incipient Drawdown Conditions in Two-Layered Stratified Flow.

AUTHOR: Subhash Gupta, B.Tech. (Mech. Eng.)

SUPERVISORS: Dr. B. Latto and Dr. D. G. Huber

NUMBER OF PAGES: x, 85

SCOPE AND CONTENT:

An experimental study of stratified fluid flow phenomena for two equal depth, different density stratified liquids in a rectangular channel is presented. Two two fluid combinations were used, a sugar water and fresh water, and fresh water and varsol. The critical value of the determined densimetric Froude number at which the upper fluid began to participate in the flow was obtained and found to be 0.28 as against Huber's (1) predicted value of 2.76. It was concluded that the interfacial mixing and viscous effects are largely responsible for this difference.

An attempt to extend Harleman's (7) work was made. The results obtained in present work were in good agreement with Harleman's (7) experimental work.

ACKNOWLEDGEMENT

The author gratefully acknowledges the help and direction of Dr. D.G.Huber and Dr. B.Latto in the planning, building and performance of this project.

This project was sponsored by the National Research Council of Canada (Grant Number 214-1348-000).

CONTENTS

NOMENCLATURE

Symbol	Description	Units
A	Orifice area	ft^2
b	Height of gate opening	ft.
c	Calibration constant of the measuring tank	ft^3/ in.
D	Pipe diameter	ft.
d	Orifice diameter	ft.
e	Percentage drawdown of the upper fluid	-
E	Percentage error in critical densimetric Froude number.	-
F_1, F_2	Densimetric Froude number of the upper and the lower fluid respectively	-
F_H	Densimetric Froude number of the lower fluid as defined and used by Harleman (5)	-
F_c	Free stream densimetric Froude number	-
g	Gravitational constant	ft/sec^2
g'	Effective gravitational constant $\left[g.\frac{\Delta S}{S}\right]$	ft/sec^2
H_1, H_2	Fluid depths far upstream in the upper and the lower fluid respectively	ft.
L	Length of the test channel (4 ft.)	ft.
p_1, p_2	Pressure in upper and lower fluid layers	lbf/ft^2
Q_1, Q_2	Volume flow rates in the upper and the lower fluid respectively	$ft^3/sec.$
K	Orifice constant	-

Symbol	Description	Units
Q_c	The critical discharge in the lower layer from Harleman's (7) analysis	$ft^3/sec.$
S_1, S_2	The specific gravities of the upper and the lower fluid respectively	-
ΔS	The specific gravity difference between the upper and the lower fluid, (S_2-S_1)	-
T	Time taken to fill the measuring tank from level X_1 to X_2	sec.
t	Time taken by the interface to rise by small amount ΔH_2	sec.
V_1, V_2	Fluid velocities far upstream in the upper and the lower layer respectively	ft/sec.
V_c	Free stream velocity of the lower fluid	ft/sec.
W	Width of the channel	ft.
X	Distance of the plane from the leading edge, i.e. starting point of boundary layer	ft.
X_1, X_2	The initial and the final water level in the measuring tank	ft.
x	Distance of the plane from the point where two fluids come together	ft.
Y	Manometer height	ft.
y_s	Viscous layer thickness at the interface	ft.

Symbol	Description	Units
α	Kinetic energy correction factor	-
ρ_1, ρ_2	Mass densities of the upper and the lower fluid respectively	$slug/ft^3$
γ_1, γ_2	Weight densities of the upper and the lower fluid respectively	lbf/ft^3
ν	Kinematic viscosity	$ft^2/sec.$
μ	Absolute viscosity	centipoise
δ	Boundary layer thickness	ft.
ψ	Stream function	-

LIST OF FIGURES

LIST OF TABLES

TEXT

1. INTRODUCTION

There is a growing interest in the capability to withdraw a selected fluid from a reservoir in which the fluid density is a function of the depth. A number of factors may cause the density variation such as, a temperature gradient, suspended sediments, dissolved salts or other chemicals.

The number of engineering fields which are concerned with the mechanism of stratified flow is fairly large. Control structures (structures made to control the flow of a selected fluid in a stratified fluid system) are being successfully used. Large reservoirs and lakes , when used as a heat sink for a thermal or nuclear plants have density stratification. It is obviously desirable to withdraw only the coolest water for efficiency reasons. Furthermore,the useful life of major structures could be increased by reducing sedimentation which could be achieved by removing water containing large amounts of suspended sediments. Control of saline water intrusion into canals or rivers by the erection of various barriers may be achieved by making use of density stratification.

In most of the cases mentioned above the fluids are incompressible,miscible, have similar viscosities and the density difference is small.

The problem of two-layered flow towards a rectangular sink of different opening sizes was considered by Harleman (5,7) in his papers. An analytical solution of the limiting case when the

sink height approaches zero,i.e. the case of line sink Fig.1.1 was presented by Huber (1), Huber and Reid attempted an experimental varification and observed that viscous wall effects were too large to be neglected.

Reid's (2) interpretation, Fig.A 3-1, failed to explain the wide scattering of the data points near incipient drawdown condition,i.e. when the upper fluid ceases to flow along with the lower fluid. Furthermore,there were insufficient data to make comparision with Harleman's work(5). Uncertainities given above led to the necessity of further work in this field.

The purpose of this research was to investigate the viscous effects on the incipient drawdown condition when,two equal depth, stratified fluids flow towards a line sink, which was the case considered analytically by Huber (1). A comparison between Harleman's (5,7) and the present experimental work is presented in this thesis.

Experimental tests were conducted with various channel widths, ranging from 2 inches to 6 inches in 1 inch increments. A sketch of the apparatus used is given in Fig. 3.3.

Problem:

The problem was to investigate experimentally the densimetric Froude number of the lower fluid at the incipient drawdown condition for varying channel widths and thus to establish quantitatively the wall effects. The configuration used was the same

as that considered by Huber (1) in his analysis.

Huber (1) in his analytical approach assumed that the two fluids were incompressible, inviscid, homogeneous and that the flow was irrotational. Huber's (1) analytical set up is shown in Fig.1.1 where V_1 and V_2 are the velocities at far unstream in the two fluids and are assumed to be of constant magnitude in their layers, H_1 , H_2 are the equal depths of the two layers far upstream and S_1 , S_2 are their specific gravities. A line sink is located at the bottom corner of the rectangular box. Further, Huber (1) assumed that pressures are common to each fluid and slip occurs at the interface.

If the fluids are at rest the interface would be horizontal. A gradual increase of flow of the lower fluid would eventually bring down the interface. When the interface reaches the line sink the critical point is reached and the upper fluid also starts flowing along with the lower fluid. A further increase in the strength of the sink will cause increase in the magnitude of the discharge rate and also change in the specific gravity of the total fluid. It is apparant that two factors are of paramount importance in determining the interfacial shape and the flow of the two fluids; inertial forces and gravity forces. Therefore, it would be expected that the densimetric Froude number would play a key role. Huber (1) defined densimetric Froude number as,

$$F = \frac{V^2}{H\, g\, (\Delta S/S)}$$

where V and H are the velocity and the depth of the layer far upstream respectively, S is specific gravity and ΔS is the specific gravity difference between the two layers.

A plot relating F_1 and F_2 , the densimetric Froude numbers for the upper and the lower fluids respectively, is shown in the Fig. A3-1. The experimental plot obtained by Reid (2) is also shown along with the theoretical plot. It can be seen that there is a uncertainity near the drawdown point which varied from F_2 =.21 to F_2 =.76. It was stated by Reid (2) that the wall effect had more influence at small widths and that by increasing the width, the theoretical value could be approached. The correctness of this prediction was tested in this experimental work.

Fig. A3-2 which is reproduced from Reid's (2) thesis shows a comparision between Harleman's (5) and Reid's (2) experimental work. The single point in the region H_2 /b =3 to 12 was considered to be insufficient to justify the nature of the curve, especially when the curve appears to be rapidly changing its nature. In order to compare Harleman's (5,7) work it was desired to find the value of the densimetric Froude number at drawdown points for different values of the ratio of the interface height to the sink height, H_2 /b .

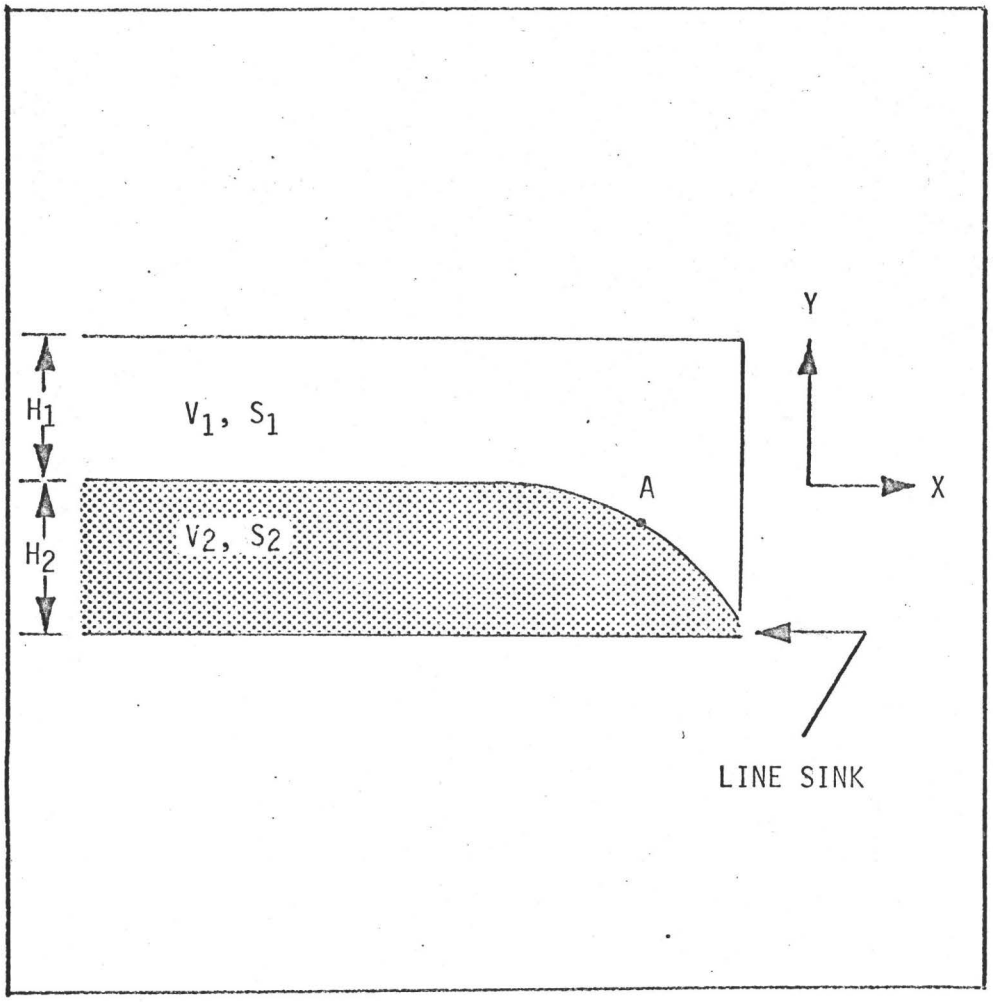

FIGURE 1.1: SCHEMATIC DIAGRAM OF THE SET-UP USED IN THIS RESEARCH.

2. LITERATURE SURVEY

Harleman (3) investigated analytically and experimentally the case for two stratified fluids in which the height of the lower fluid was limited. The intake was located at a bottom boundary, as shown in Fig.2.1. Only the lower fluid was withdrawn until the incipient drawdown was reached. This was the condition when the upper fluid commences to take part in total flow. Different arrangements of intake configuration , including full round, half round and re-entrant types, were studied. These changes in intake configurations were found to have negligible effect on the efflux velocity. The efflux velocity equation, verified by Harleman's(3) analytical and experimental work is,

$$V_e/(g'Z_o)^{\frac{1}{2}} = 2.05\ (Z_o/D)^2$$

Rouse and Davidian (4) carried out an experimental study of two stratified fluid layers being withdrawn from the circular intake pipe located above an interface as shown in Fig.2.2. The purpose of the study was to determine experimentally, the rate of flow necessary to develop a waterspout to the point at which the upper as well as, the lower fluid is carried into the pipe. Their investigation considered two two fluids combinations ; air and water,and fresh water and saline water (specific gravity 1.1). From the results thus obtained , they established the following relation,

$$V_e/(g'Z_o)^{\frac{1}{2}} = 5.70\ (Z_o/D)^{1.5}$$

Harleman, Gooch and Ippen (5) studied a two fluid flow in an attempt to obtain the maximum possible discharge rate for flow only from the lower layer, for various values of H_2/b; H_2 and b being the interface elevation and the gate opening respectively, Fig.2.3. The theoretical analysis was based on the one dimensional energy equation. It was necessary to account for the non-uniformity in both the velocity distribution and the hydrostatic pressure distribution in the plane of the vertical gate. Khafagi Hammad (21) studied departure from the hydrostatic condition due to stream line convergence. A critical densimetric Froude number relationship for the lower layer was obtained as a function of the ratio H_2/b and the kinetic energy factor α . The kinetic energy correction factor is a factor which, when applied to the kinetic energy term found by using the average velocity over a section, will determine the average kinetic energy passing that section. Although no attempt was made to measure this kinetic energy correction factor due to the three dimensional character of the flow and the low velocities involved, laboratory tests have verified the curves for high values of kinetic energy correction factor. Results obtained are shown in Fig.2.4.

Elder and Dougherty (6) have reported some control structures , which were made using a stratified flow analysis. A skimmer wall was constructed to utilize colder water for a condenser in the Kingston Steam Plant of the Tennessee Valley Authority. A comparision of field data before and after

construction of a skimmer wall, as well as, the effect of an under-water dam was made and a reduction in the water temperature, as high as 20^{o} F, was observed. The cost analysis of the project clearly indicated the feasibility of such a type of structure being used successfully in practice.

Harleman and Elder (7) extended Elder and Dougherty's (6) research on the Kingston Steam Power Plant by determining the maximum available condenser water. For a plane skimmer wall the maximum discharge from the lower layer, without simultaneous flow of the upper layer was shown to be given by,

$$Q_c = W \left(g' \left(2/3 . H_2 \right)^3 \right)^{\frac{1}{2}}$$

In order to achieve the maximum discharge from the lower layer, the ratio of the interface elevation to the skimmer wall opening H_2/b , was given as 2.5. For a radial wall the same discharge equation was found to apply provided W is interpreted as the wetted perimeter of the wall. In this case the ratio H_2/b may be reduced to 1.5. The theoretical and experimental results are shown in Figs.2.5 and 2.6.

Angelin and Flikested (8) developed the intake configuration for cooling water supply from stratified sea-water. The problem of density current flow was first treated theoretically, both generally and also for the given conditions. On the basis of these calculations a scheme for the intake structure was

designed. Model tests were carried out to verify the methods of calculation employed and also to study the design of the intake configurations.

Bata (9) considered the problem of circulation of cooling water in thermoelectric power plant. Analytical and experimental investigations show that among many factors the most important are the channel depth, the discharge rate, the distance between intake and outlet, the degree of heating of diverted water, and the relative amount of diversion of outlet water.

Macagno and Rouse (10) carried out an analytical and experimental investigation of the interfacial mixing in the stratified flow. A plot of Reynolds number against Froude number indicated that the laminar regime was confined to a rather small zone.

The velocity distribution in the laminar boundary layer formed at the interface between two stratified liquids of different densities and viscosities, was given by Keulegan (11). An approximate numerical method,which was employed, was reasonably accurate on a second order approximation.

Potter (12) extended Keulegan's(11) work to the case when both fluids are moving but at different velocities and obtained approximate numerical solutions using a sextic polynomial.

Wood (13) has investigated the case of a hydraulic jump occuring when a fluid is flowing under a stationary less dense

fluid. Remarkable similarity between the hydraulic jump under such conditions and a free surface hydraulic jump was demonstrated.

The occurence of velocity concentration or jets was pointed out by Long (14). Movement of the stratified fluid around the obstacles revealed multiple jet phenomena and fundamental observations indicated that the width of the jets tended to take a value such as to make the internal Froude number, based on the width, of the order of one.

Comparatively little work has been done for the continuous density gradient case, as compared to the two fluid systems. This is not surprising because the two fluid systems are relatively simpler to treat analytically, and in many cases they represent a reasonable approximation to the physical situation.

Yih (15) has pointed out that the flow of an irrotational inviscid stratified fluid with continuous density gradient could be treated as a limiting case of a multilayered system. Treatment of this type of flow discharging at a line sink formed by the channel bottom and vertical wall,has led to the conclusion that, in the absence of gravity, steady fluid flow corresponds to stratified flows, the velocity of which is simply that for irrotational flow divided by the square -root of the density. The gravity effects can be neglected only for the horizontal flows or for high densimetric Froude number conditions. Yih(15)

has also shown that in such cases at a remote distance from the sink an exact analytical solution can be obtained, which indicates that the fluid cannot be separated in two parts if the densimetric Froude number is greater than $1/\pi$.

Yih (16) has also shown a method for constructing potential flows of two fluids having a common interface. He discussed the stability of periodic disturbances present in a parallel flow with continuous density gradient.

Debler (17) experimentally investigated the discharge of a stratified fluid, having a stable linear density variation upstream, through a horizontal slot at the lower end of a channel. The densimetric Froude number in this case was defined as,

$$F = (q/h^2)(h\rho_0/g\,\Delta\rho)$$

where,

q = slit discharge per unit width

h = total depth of fluid

ρ_0 = density at channel bottom

$\Delta\rho$ = density difference between top and bottom layer

He demonstrated that for such cases a critical densimetric Froude number appeared to exist, which is in agreement with Yih (15), below which the flow divides into two distinct regions. These are an upper region composed of fluid that did not flow into the sink and which remained relatively motionless and a

lower region in which all the discharge was concentrated. The variation of the height of the region of discharge with the densimetric Froude number was found to be 0.28 as against $1/\pi = .32$ which was predicted by Yih (15).

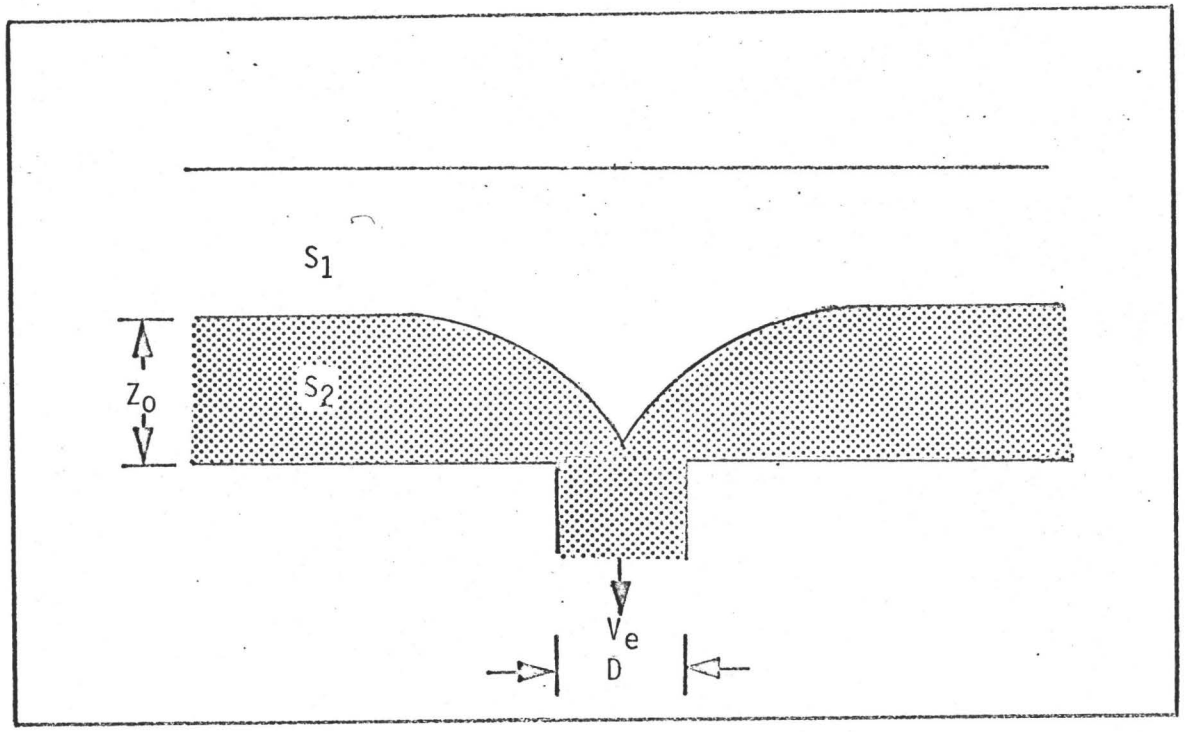

FIGURE 2.1: SCHEMATIC DIAGRAM OF THE SET-UP USED BY HARLEMAN(3)

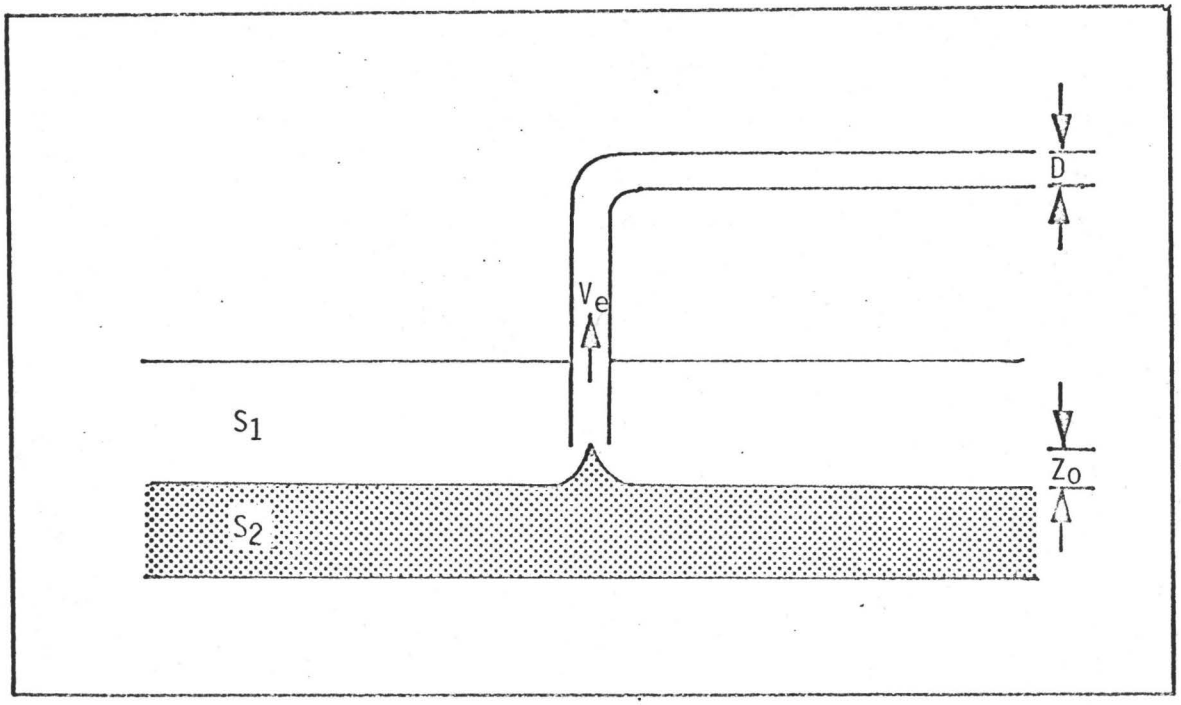

FIGURE 2.2: SCHEMATIC DIAGRAM OF THE SET-UP USED BY ROUSE AND DAVIDIAN (4).

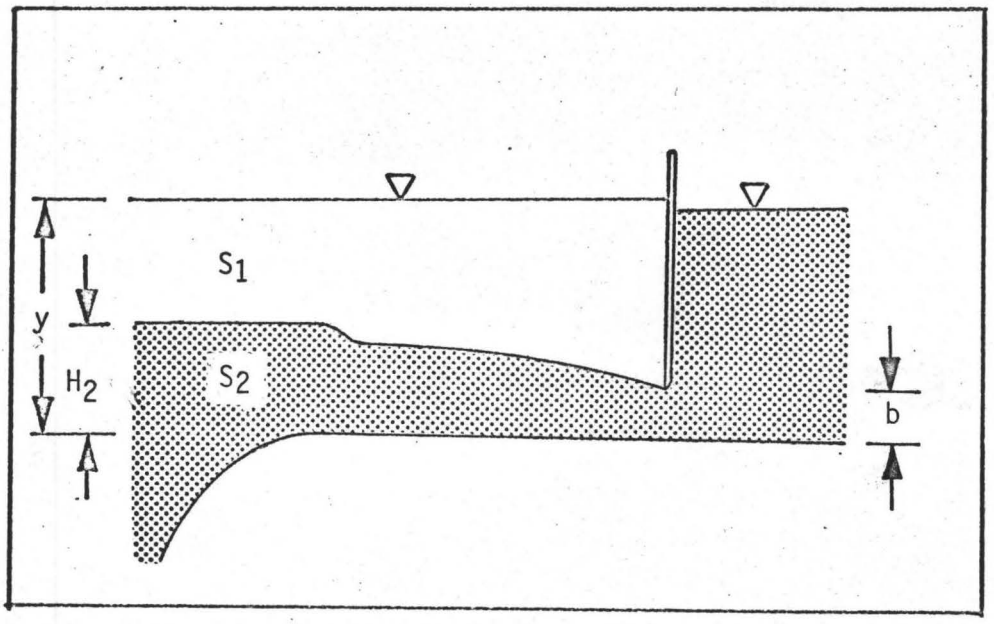

FIGURE 2.3: STRATIFIED FLOW CONTROLLED BY A SUBMERGED SLUICE.

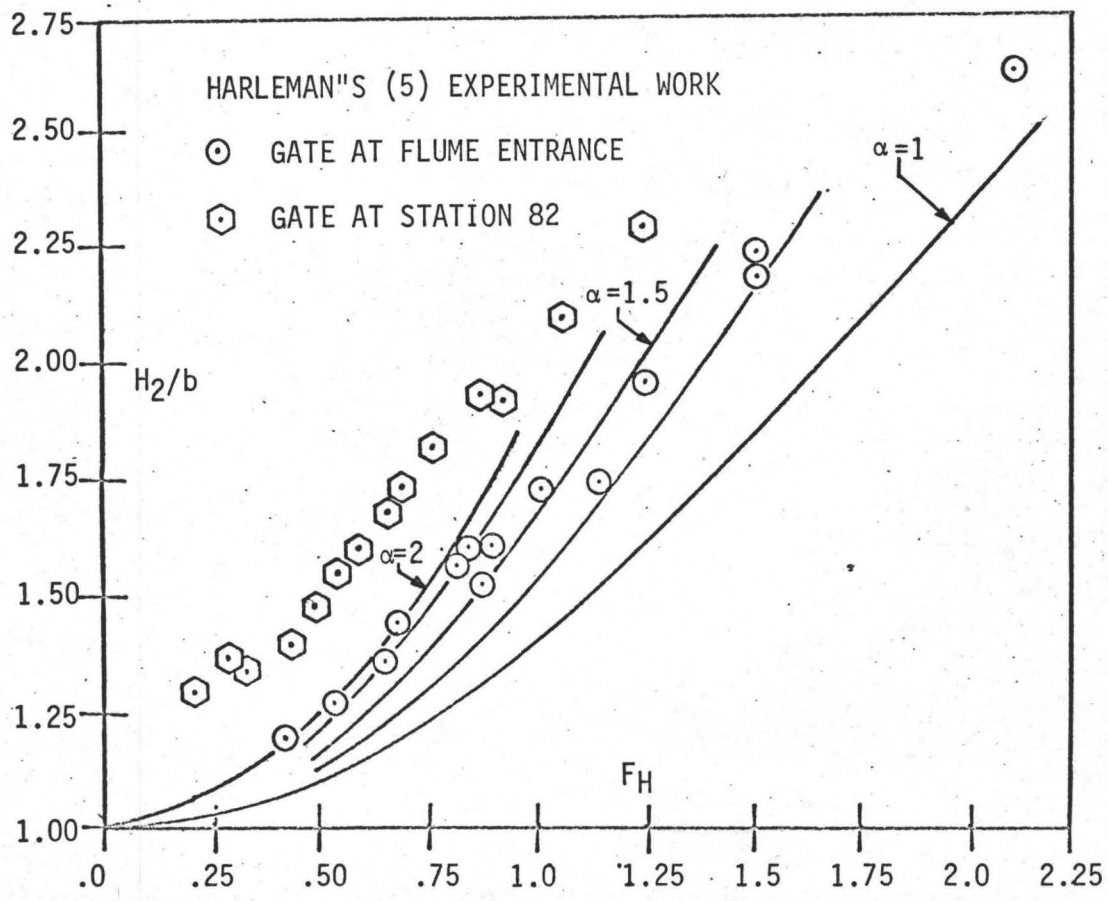

FIGURE 2.4: SLUICE CHARACTERISTICS AT INCIPIENT DRAWDOWN

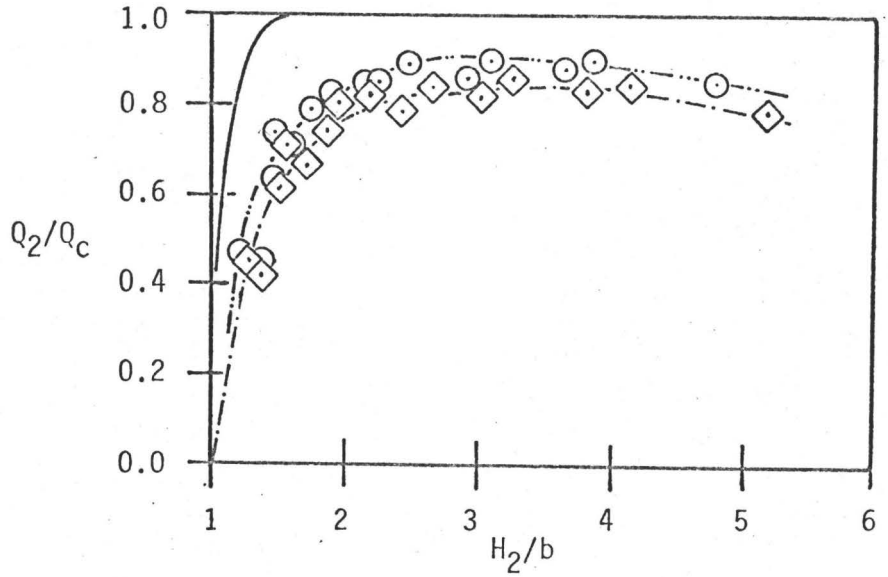

FIGURE 2.5: PLOT OF HARLEMAN'S (7) ANALYTICAL AND EXPERIMENTAL WORK FOR A PLANE SKIMMER WALL.

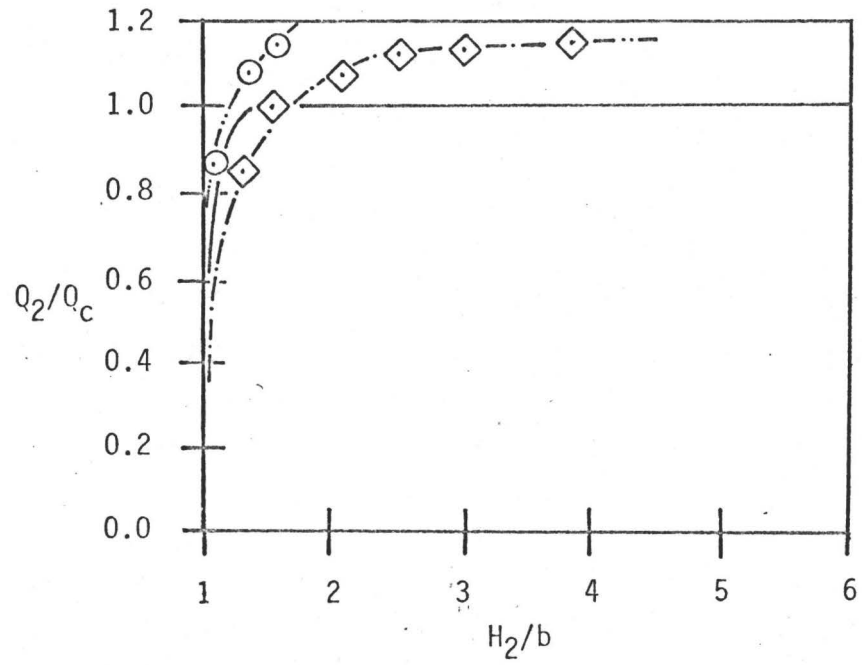

FIGURE 2.6: PLOT OF HARLEMAN'S (7) ANALYTICAL AND EXPERIMENTAL WORK FOR A RADIAL SKIMMER WALL.

3. TEST FACILITY

The apparatus used in the present work was designed to examine the influence of the walls on critical densimetric Froude number. The apparatus was specially designed to investigate the value of the critical densimetric Froude number where as Reid's(2) apparatus was designed to experimentally investigate Huber's (1) theoretical work.

A photograph of the test facility used is shown in Fig. 3.1. A schematic labelled diagram of the facility is shown in Fig.3.2.

Two fluids of slightly different density and approximately similar viscosity, were required to satisfy the requirements of the research. A sugar water solution and fresh water combination was selected for reasons of economy, convenience,corrosion prevention and lack of toxity. The sugar water solution was coloured with blue vegetable dye.

The test facility could be considered to be comprised of three sections, a test section, piping and pump set, and a flow measuring orifice.

3.1 Test Section:

This was comprised of three parts ; an entrance plenum chamber, a rectangular test channel and a sink chamber. The test liquid was supplied to the plenum chamber through a diffuser which was used to slow down the incoming fluid.

A dividing plate,as shown in Fig.3.3, served the purpose of avoiding any pre-mixing which could have occured. It also acted as a guide plate for the sugar water solution.

A flexible pipe was connected to the tank above the dividing plate for the purpose of filling the system above the sugar solution, with fresh water. A header tank was connected to the main entrance plenum chamber to maintain sufficient pressure in the system. A glass tube was attached to the header tank in order that level of the fresh water could be read.

The test channel had a stabilizing zone which was sufficient to allow the flow to stabilize without mixing. The channel width was altered by replacing different back plates, each for a particular channel width. The dividing plates were also replaced each time, so as to fit different back plate shapes. Drawings of the back plates and dividing plates are shown in Fig.3.4.

The main test section included several "Swage-Lok" fittings at suitable locations for injection or sampling purposes. A probe was inserted from the top of the channel for taking samples near the interface. The front wall was made of plexi-glass for flow visualisation. A transparent plastic sheet having grid lines on it, was attached to the front wall. The back wall of this section could also be moved in order to attain different channel widths.

The test section had a sliding gate which could be adjusted

to give a required sink height. The flow discharged into a sink chamber, which had a movable back wall, similar to that of test section, and a transparent plexi-glass front. Pet-cocks were positioned at suitable locations to act as air bleeds.

3.2 Piping and Pump Set:

In order to keep velocities sufficiently low enough to avoid excessive turbulence, 4 inch pipes, pipe fittings and gate valves were used throughout the system.

In order to obtain a wide range of flow rates at any pressure, it was desirable to choose a positive displacement pump. A Viking E.Q.* pump which was capable of delivering from almost zero to a maximum of 200 U.S. gallons per minute was used for this purpose.

A 3 H.P., 220V D.C. motor was used to drive the pump. The D.C. voltage was obtained by A.C.-D.C. converter. The motor speed was reduced by a compound pulley system to obtain a sufficiently high starting torque.

The pipe layout was designed in such a way so as to make it possible to achieve different flow circuits. A 3/4 in. by-pass between the pump discharge and the orifice plate was installed to divert any extra solution, whenever desired, from the closed flow circuit.

A 34" X 32" X 28" mixing tank was used for mixing and storing the sugar solution.

---

* Manufactured by Viking Pump Co. of Canada Limited, Windsor, Ontario.

3.3 Flow Measuring Devices:

An orifice meter was used to measure the sugar solution flow rate. The orifice design details are given in Appendix-1. Locating pegs were fitted on both flanges to position the orifice plate.

A mercury U-tube manometer was used to measure the pressure difference across the orifice. Orifice plates having diameters of 1/2", 3/4", 1", and 1¼" were used and are called number 1,2,3,4 respectively.

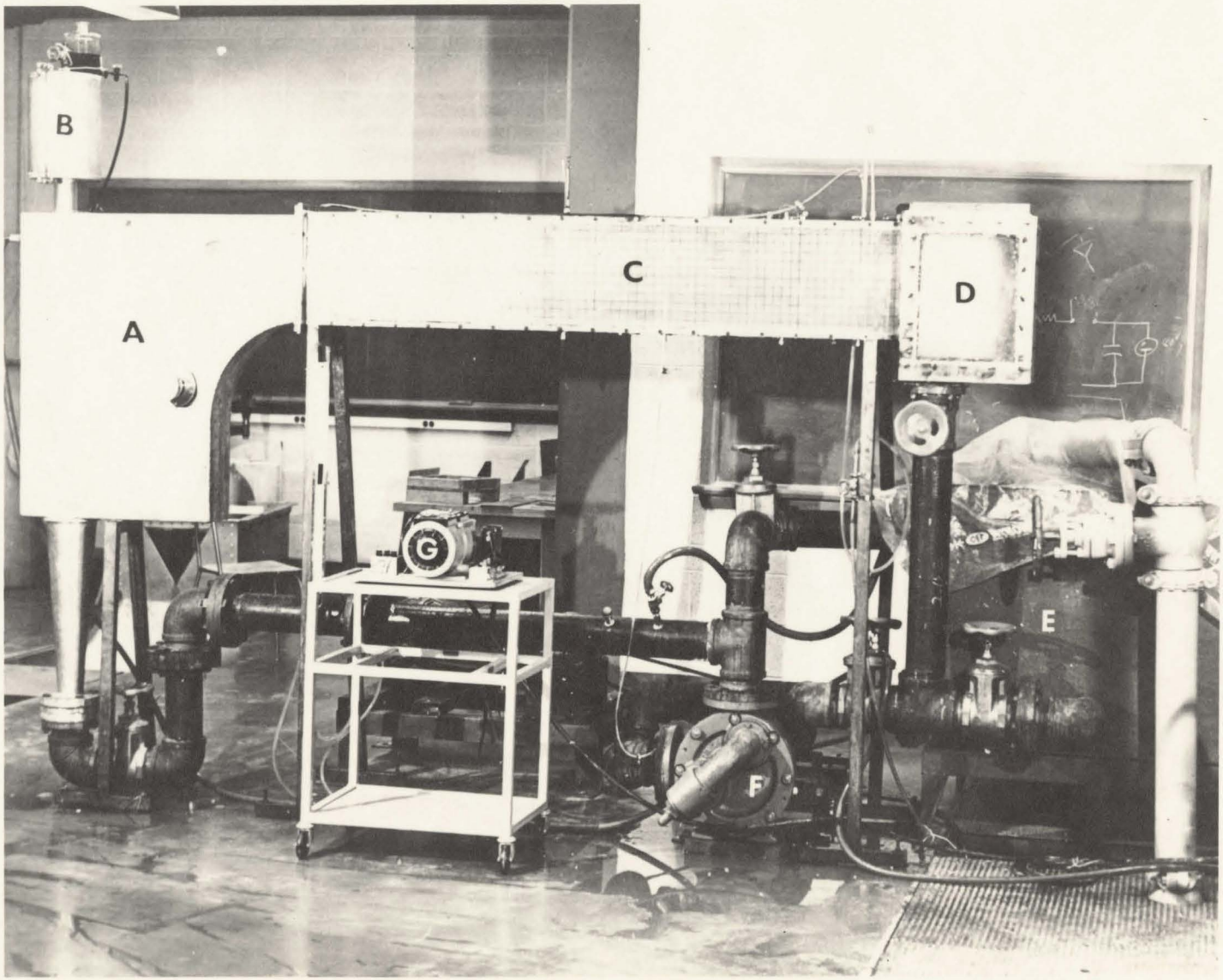

FIGURE 3.1: TEST FACILITY

FIGURE # 3.1

TEST FACILITY

A. Entrance Plenum Chamber

B. Header Tank

C. Test Channel

D. Sink Chamber

E. Mixing Tank

F. Pump

G. A.C.-D.C. Converter

I. U-Tube Manometer

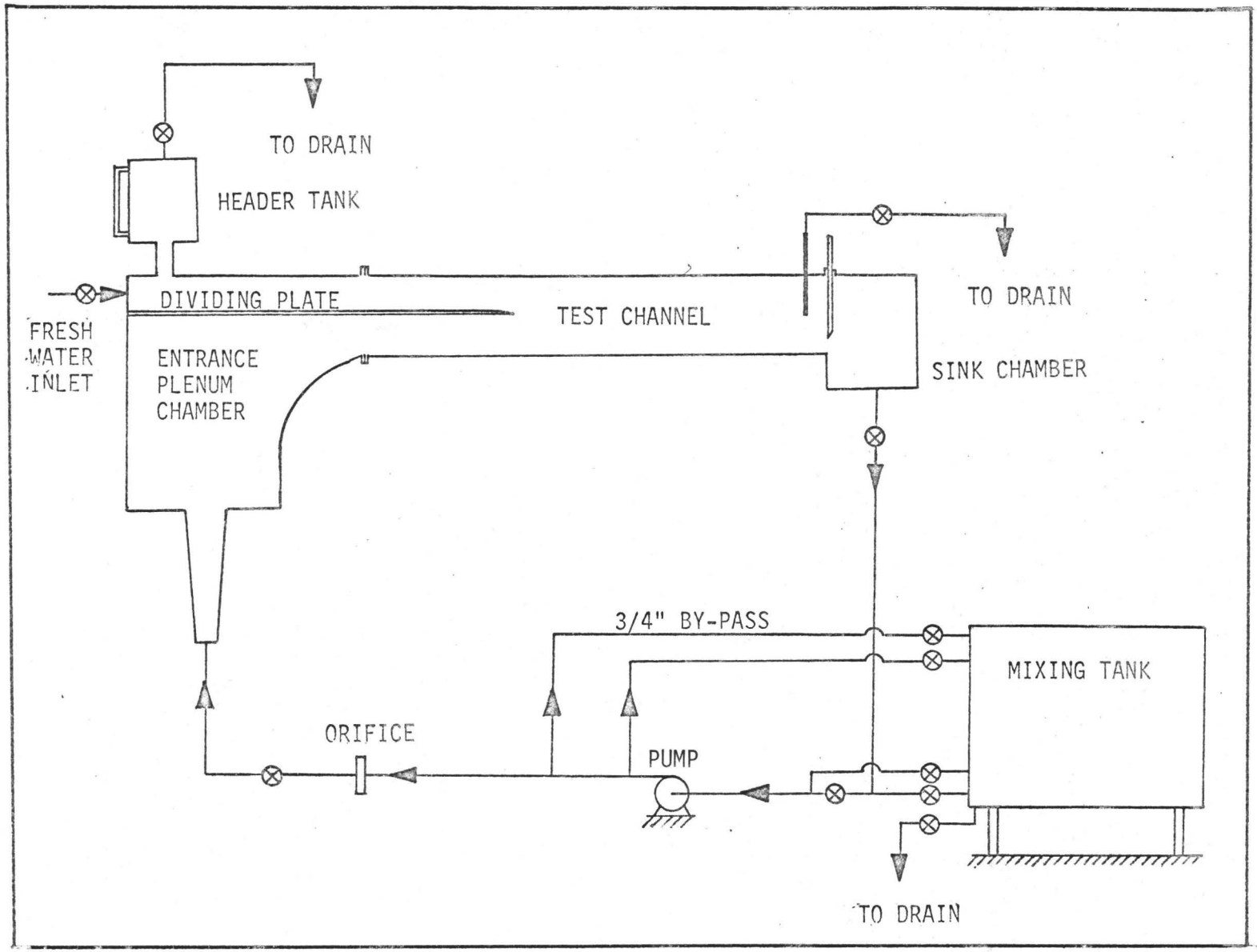

FIGURE 3.2: SCHEMATIC DIAGRAM OF THE TEST FACILITY

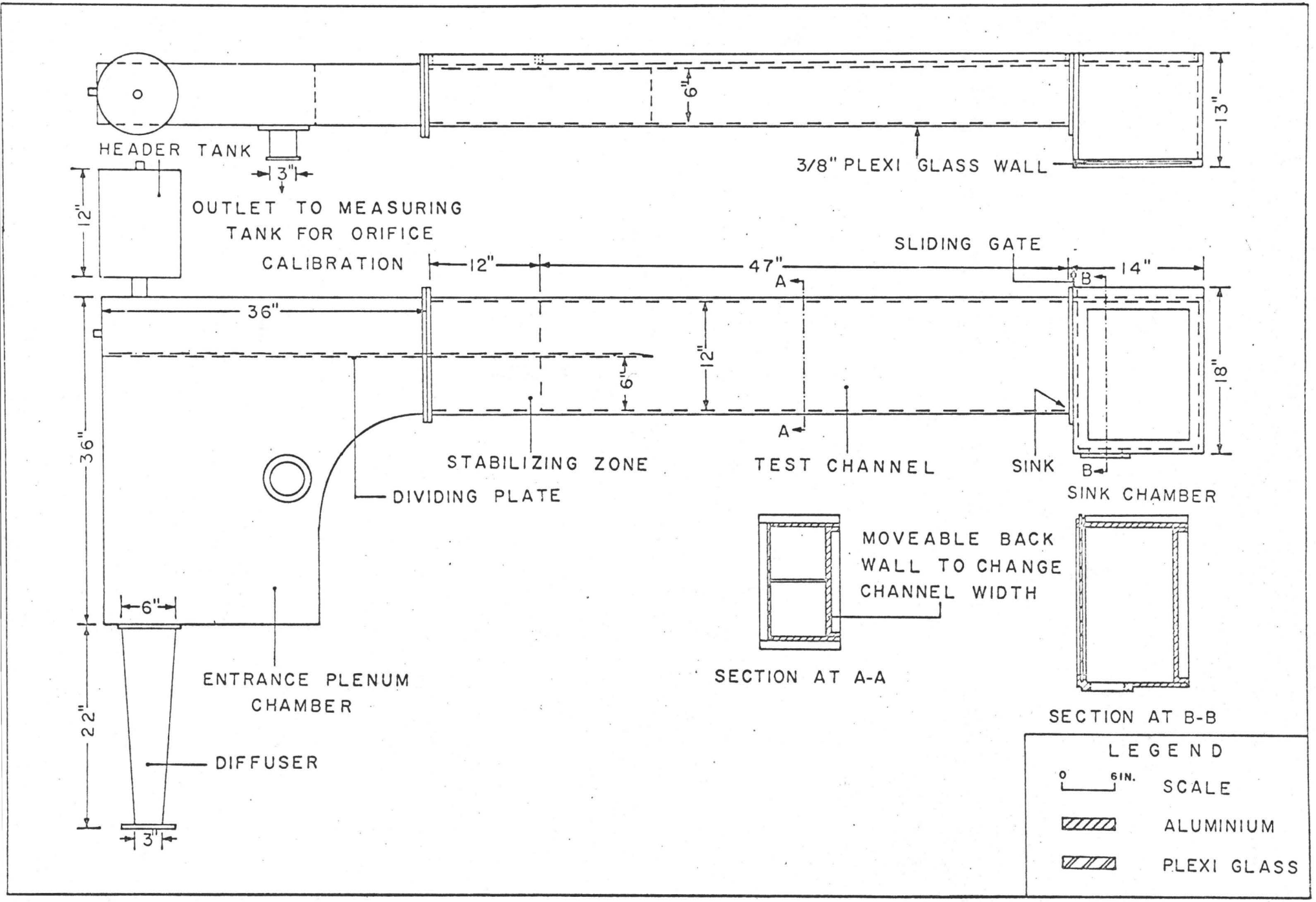

FIGURE 3.3: DETAILED DIAGRAM OF THE TEST SECTION

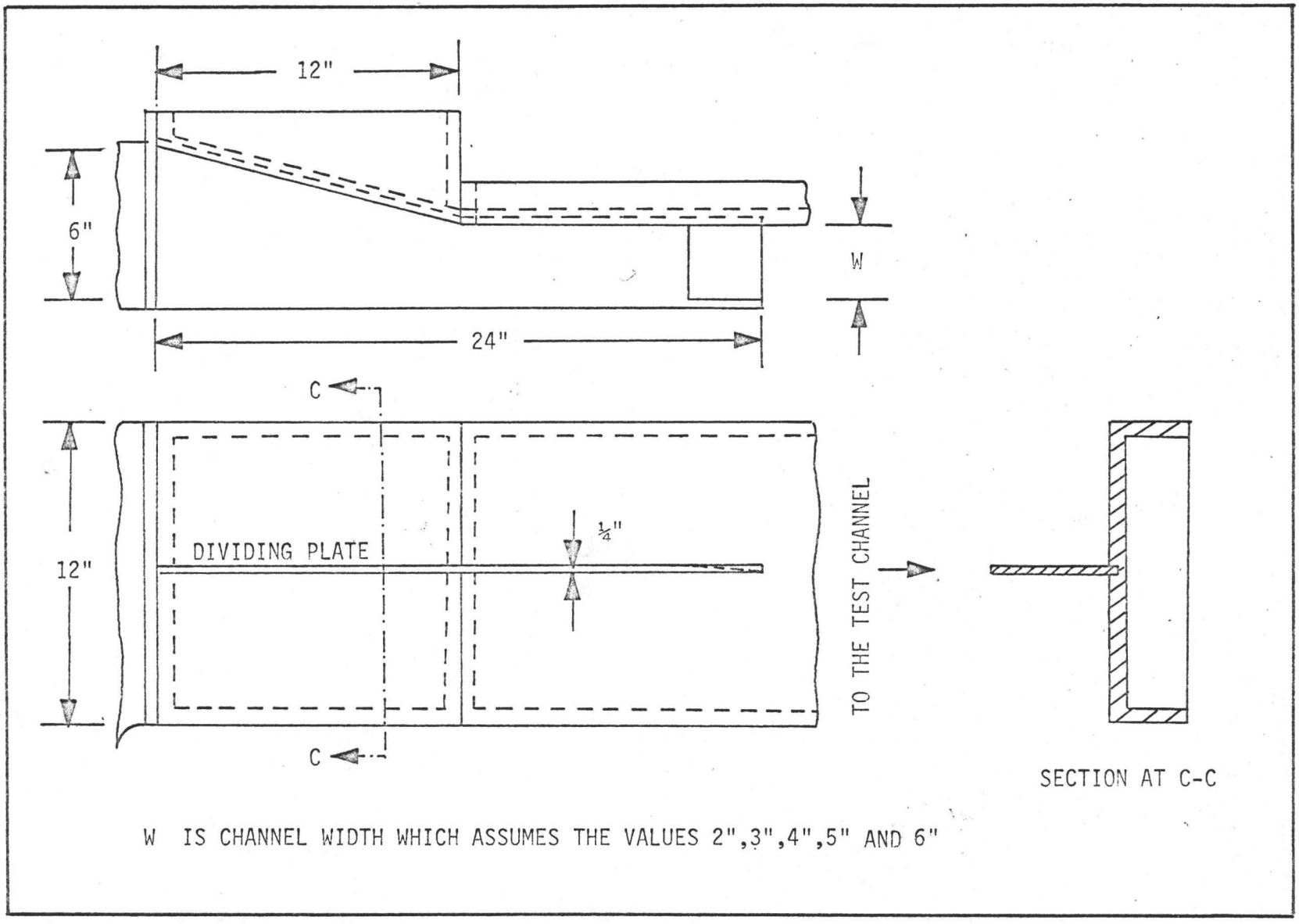

FIGURE 3.4: CHANNEL WIDTH REDUCTION ARRANGEMENT

4. TEST PROCEDURE

At the start of each experimental run, the test section was initially partly filled with the sugar water. It was necessary to drain off some of the sugar solution in order to bring down its level to the mid height of the test section. The fresh water was added in small amount through the inlet. Water ran over the dividing plate and gently issued over the sugar solution without any mixing. While filling the test section the identifiable interface level gradually dropped, because some of the sugar solution flowed to the sink chamber .

The main pump was started very slowly to avoid any ripples or waves at the interface and then slowly speeded up to the required speed. After some time the interface level started rising. No further increase in pump speed was made when the interface level approached anywhere near to the mid height. A stop watch was started when the fairly constantly rising interface reached mid height. The time for the interface to rise 1/8" from mid height was noted. At this point the U-tube manometer was read and samples of the sugar solution were taken at suitable points, which were 5", 2" and 0" above the bottom of the test section, to check against any possible stratification. The various samples taken at different heights before and after the drawdown condition indicated that there was not any appreciable stratification in the lower layer. The pump speed was

slowly reduced and the run was completed. With all the information available the percentage drawdown was calculated as shown on page 28 . If the percentage drawdown was between 1% to 1.5% the run was considered to be valid. That is, if 1% to 1.5% drawdown was chosen to indicate the incipient drawdown condition. For the next immediate run the sugar solution was drained off by opening the by-pass until the interface dropped down to approximately 1" to 2" below its original level.

The density of the sugar water samples was calculated by weighing them in a specific gravity bottle and comparing the value with that of distilled water.

For different manometer heights the amount of the flow rate (Q_2) was read from the calibration curve of that particular orifice. Q_2 was corrected to take into account the specific gravity difference between the sugar solution and water used for calibrating the orifices. The densimetric Froude number was calculated using the corrected Q_2, that is,

$$Q_2 \text{ (corrected)} = Q_2 \left(S_{water}/S_2 \right)^{\frac{1}{2}}$$

and

$$F_2 = \frac{(Q_{2c}/ W.H_2)^2}{H_2.g(S_2-S_1)/S_2}$$

Tests were also run for a two fluids combination of varsol and fresh water using the same filling procedure as described above. It was possible to notice drawdown visually in this case. That is, when interface drops to sink height. The results of this case are also included in later sections.

5. RESULTS

For each channel width (W), approximately 40 tests were run. However, only a few of them were considered valid because others did not confined to the 1% to 1.5% drawdown limits.

Knowing the time (t), taken for the interface to rise a small amount ΔH_2, the volume flow rate of the upper fluid (Q_1) , the percentage flow rate of the upper fluid was calculated from,

$$Q_1 = (\Delta H_2 . W . L) / t$$

and, therefore,

$$e = (Q_1/Q_2) \times 100$$

All the results are tabulated in tables 5.1 to 5.5 which give the densimetric Froude number and percentage drawdown. The results are arranged to have the Froude numbers in increasing order of magnitude. The mid value of a set of data was chosen as a representative value. The critical densimetric Froude numbers plotted against channel width as shown in Fig.5.5. It can be observed that there appears to be a limiting value at a densimetric Froude number equal to 0.28.

Table 5.6 shows the relation between the critical

densimetric Froude number F_H , as defined by Harleman (5), and Q_2/Q_c , which is the ratio of the flow at incipient drawdown (Q_2) to the critical flow calculated from the analysis (Q_c). The results are plotted in Figs. 5.6 and 5.7 along with Harleman's (5,7) analytical and experimental curves for the 1% and 2% drawdown cases.

The observed interfacial mixing is shown in Fig.5.9 where the relative density difference is plotted at various depths near the interface.

Fig.5.8 shows the critical densimetric Froude number F_2 as plotted against H_2/b , the ratio of the lower layer depth and the sink height.

The viscosities of sugar water of different specific gravities are shown in Fig.5.10 as obtained from standard hand books (19,20).

As the flow rate in the lower layer was increased the interfacial disturbances also increased. Interfacial waves moving towards sink can more clearly be seen in the case of fresh water and varsol. These waves break themselves when they reach near the sink, where the interface starts curving downwards.

A wedge shape vortex was observed at the interface near the sink where the interface started curving downwards. A similar observation was reported by Harleman (5). Apart

from this wedge shape vortex there were other noticiable vortex pattern set up in the upper fluid including primary and secondary vortices.

Results of the case using fresh water and varsol are tabulated in Table 5.7. Tests were run with two channel widths, that is, 6" and 2".

Reynolds numbers corresponding to various flow velocities of the lower fluid are also included in all tables. The hydraulic diameter for the channel flow was computed as follows,

$$\text{Hydraulic Diameter} = \frac{4.\ \text{Flow Area}}{\text{Wetted Perimeter}}$$

$$= \frac{2.\ W.\ H_2}{(\ W+H_2\ )}$$

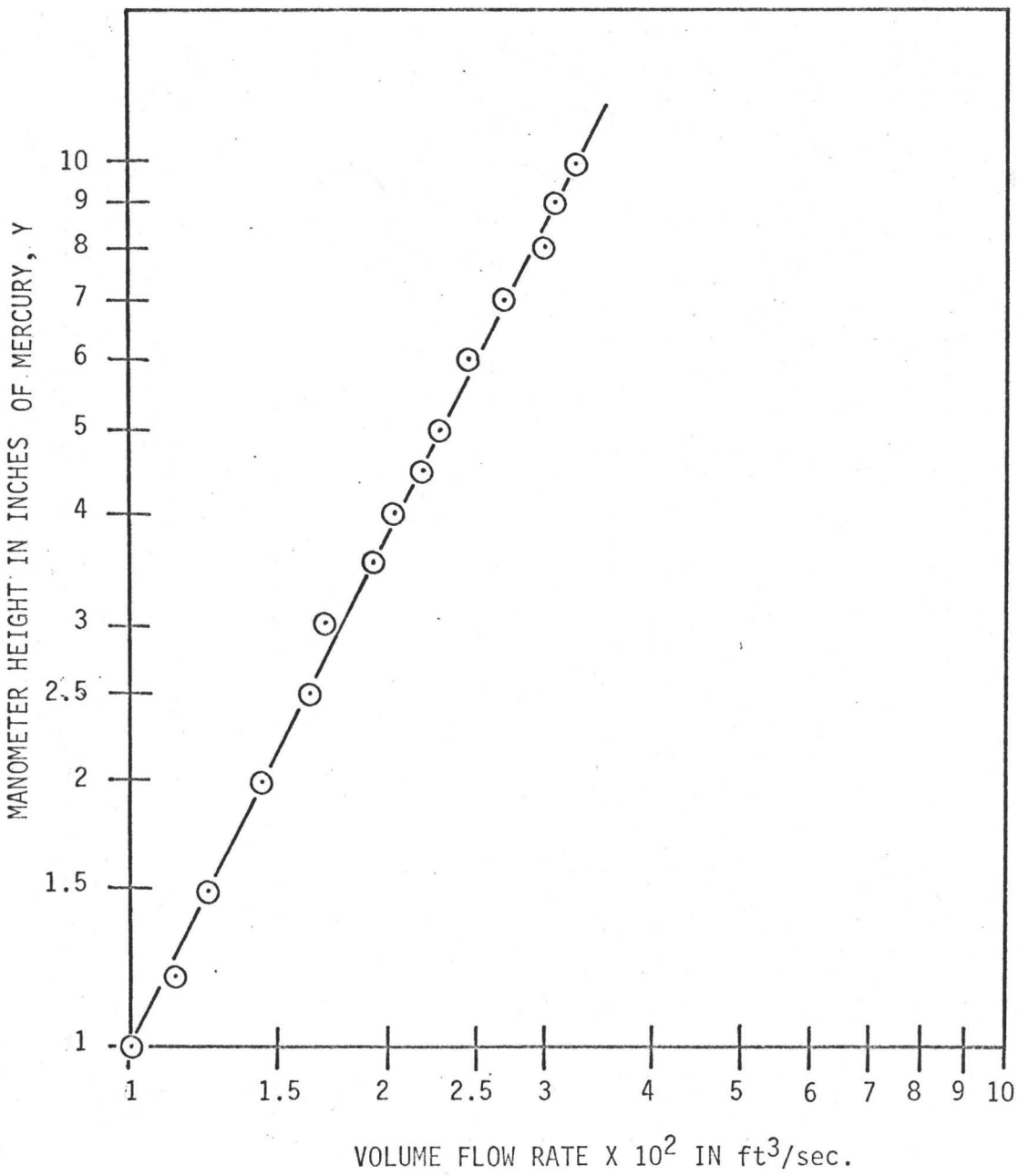

FIGURE 5.1: CALIBRATION CURVE OF ORIFICE #1

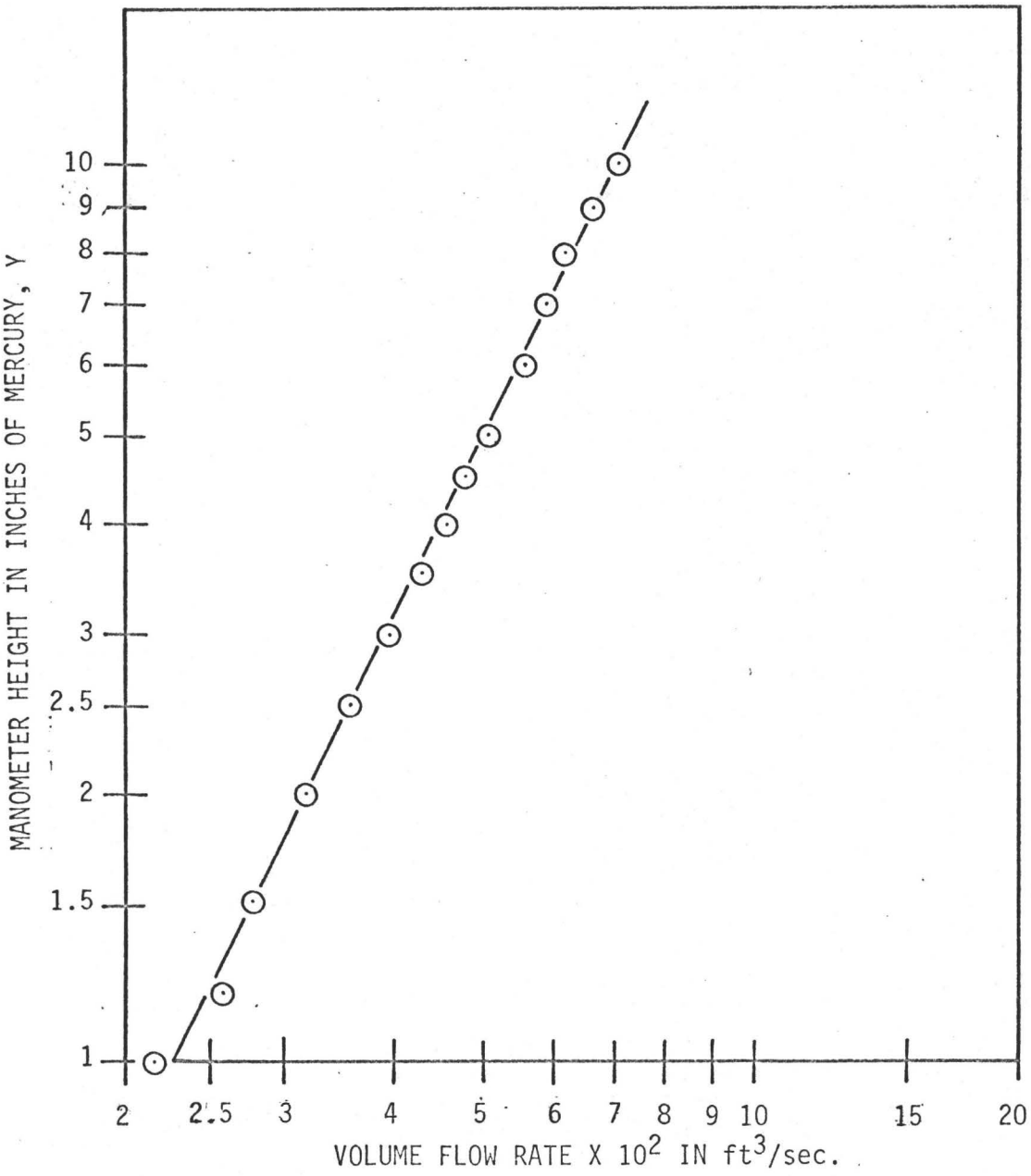

FIGURE 5.2: CALIBRATION CURVE OF ORIFICE #2

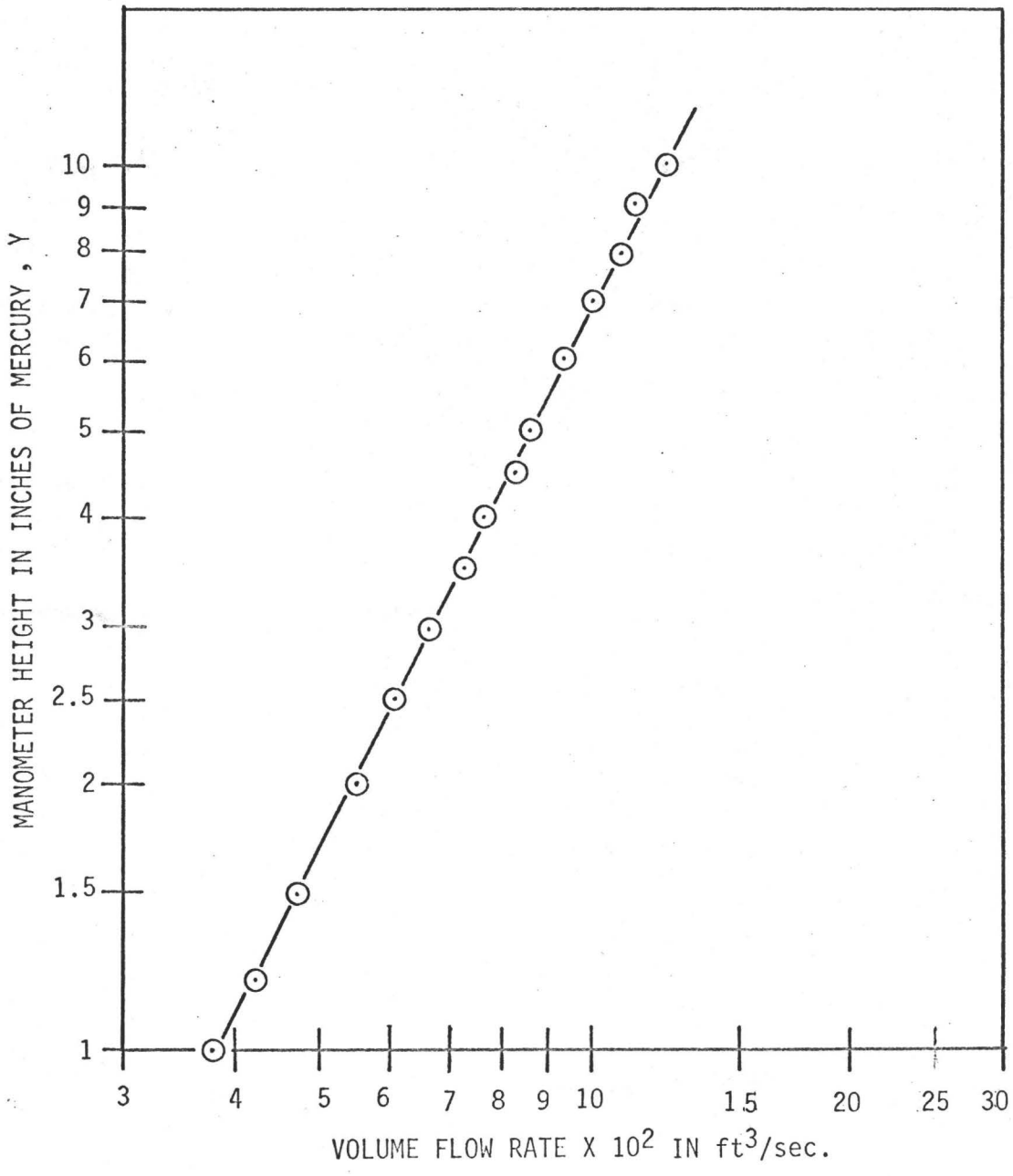

FIGURE 5.3: CALIBRATION CURVE OF ORIFICE #3

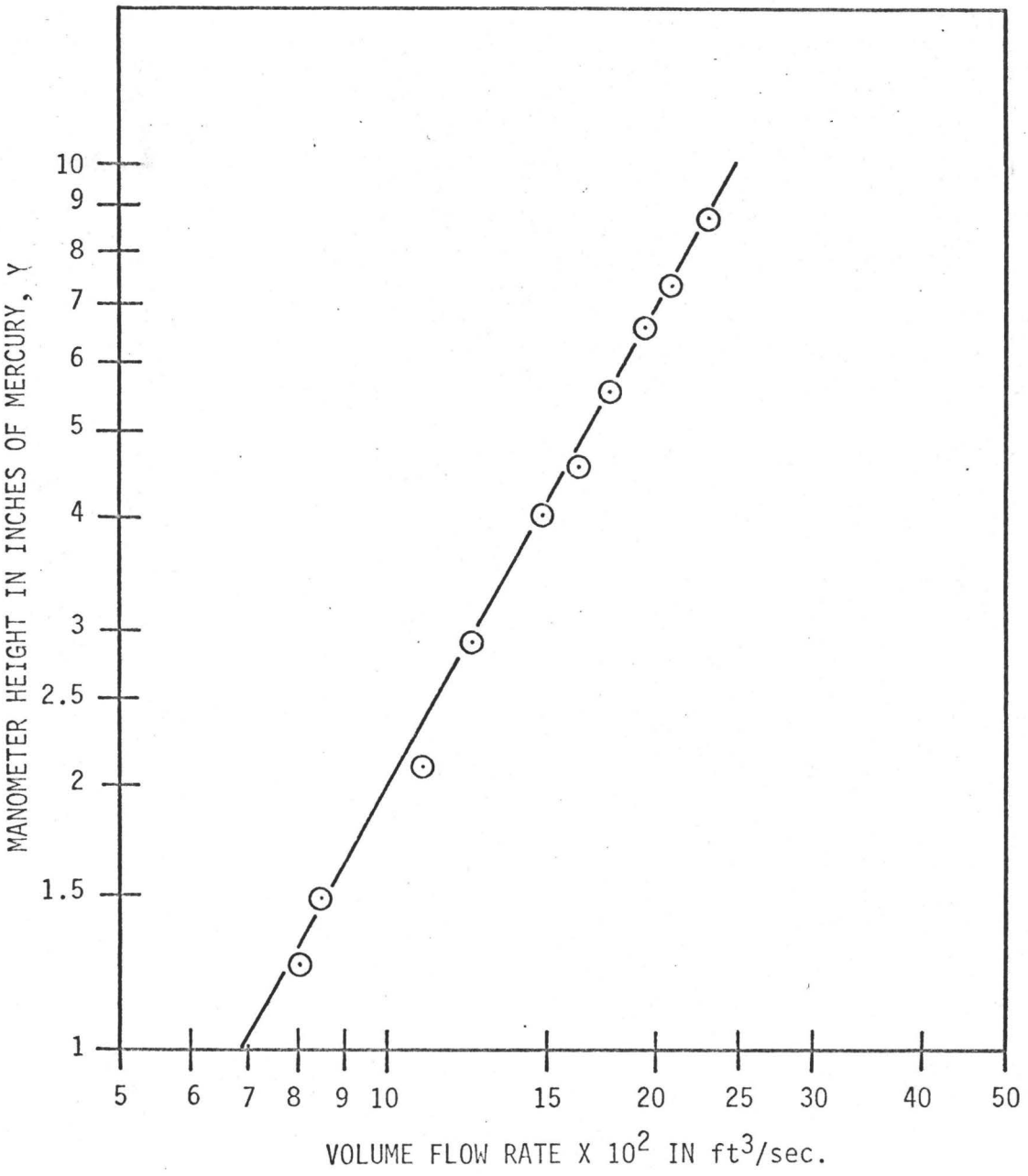

FIGURE 5.4: CALIBRATION CURVE OF ORIFICE #4

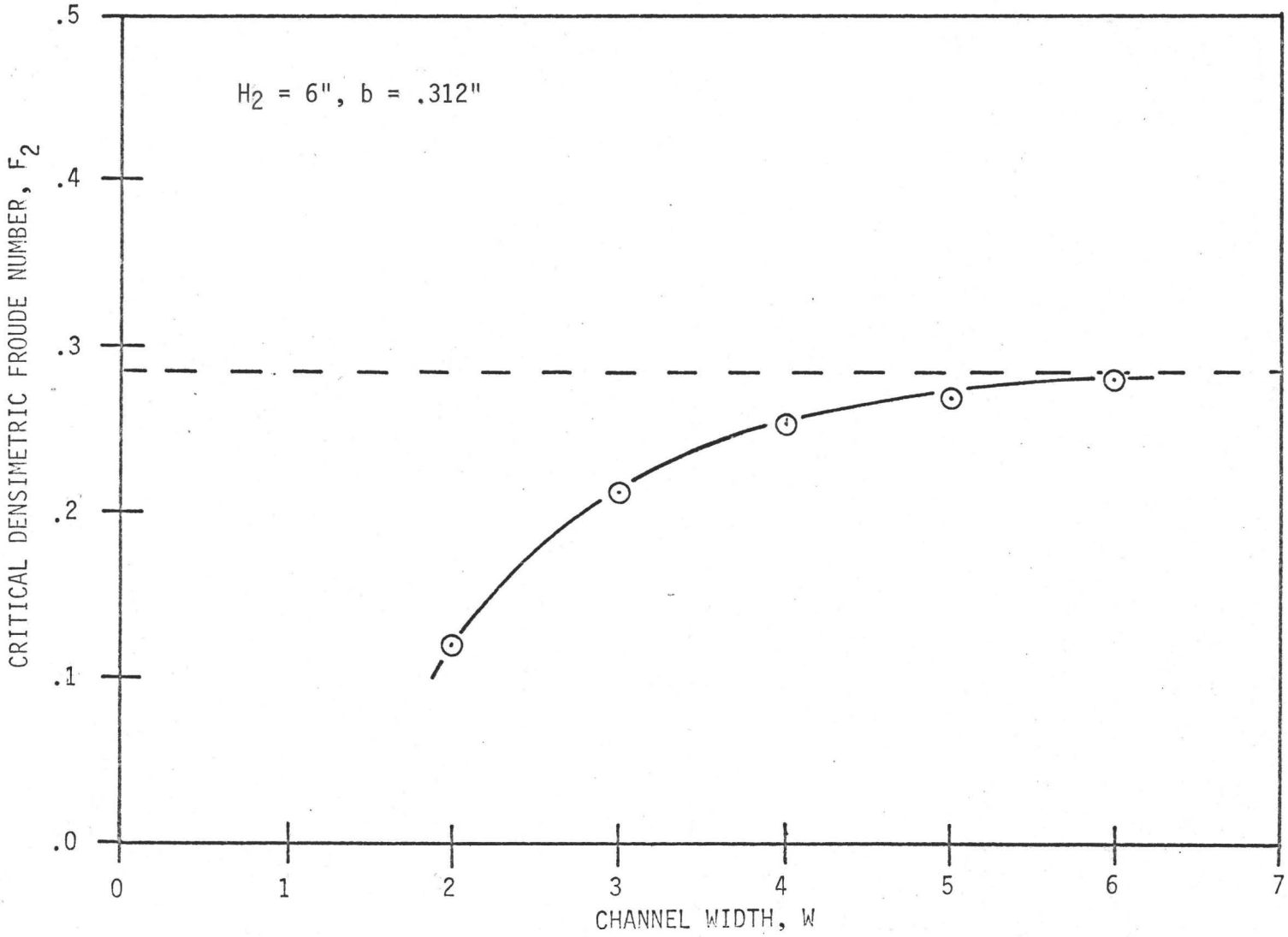

FIGURE 5.5: EFFECT OF CHANNEL WIDTH ON CRITICAL DENSIMETRIC FROUDE NUMBER, F_2

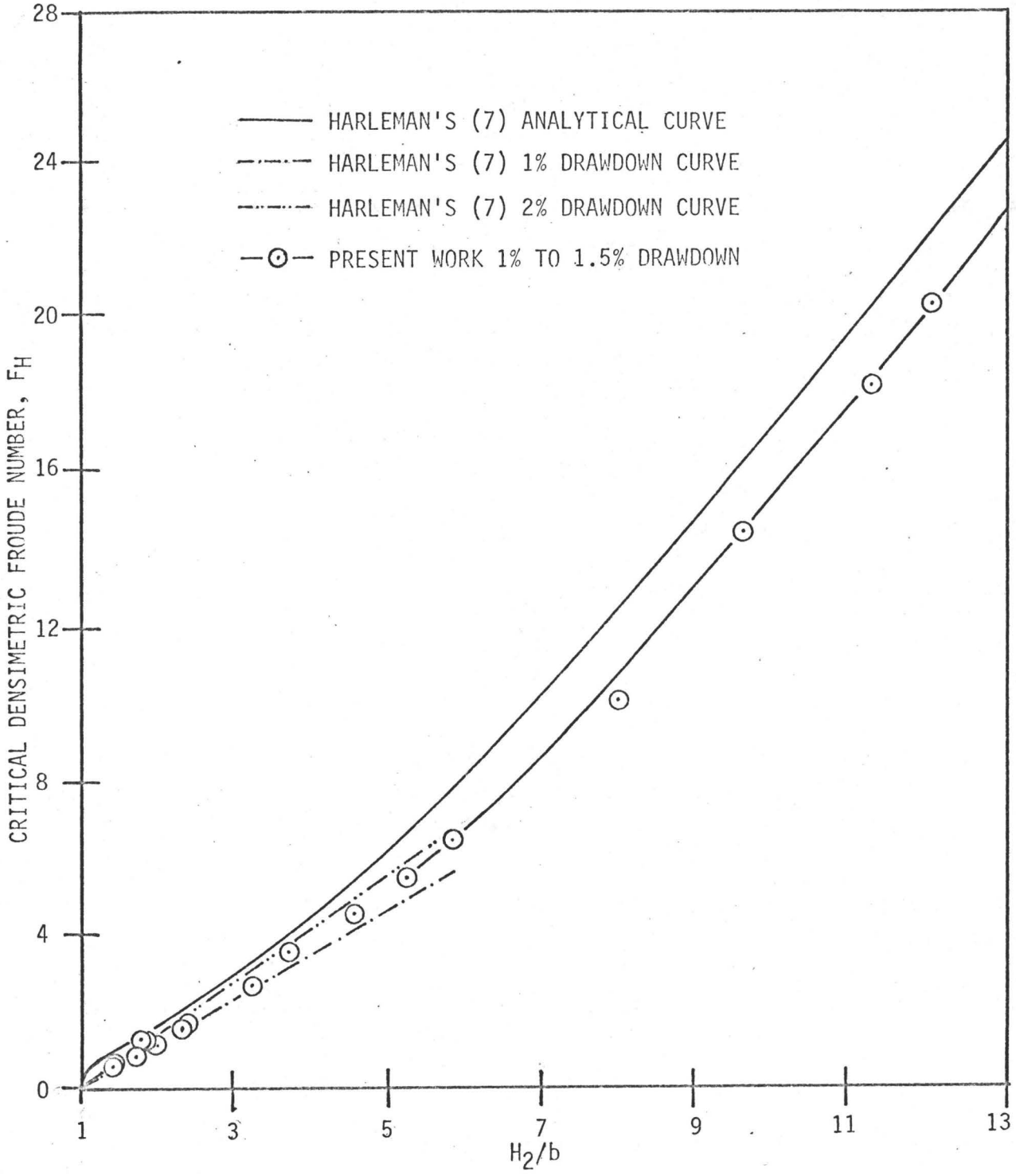

FIGURE 5.6: CRITICAL DENSIMETRIC FROUDE NUMBER, F_H vs. H_2/b.

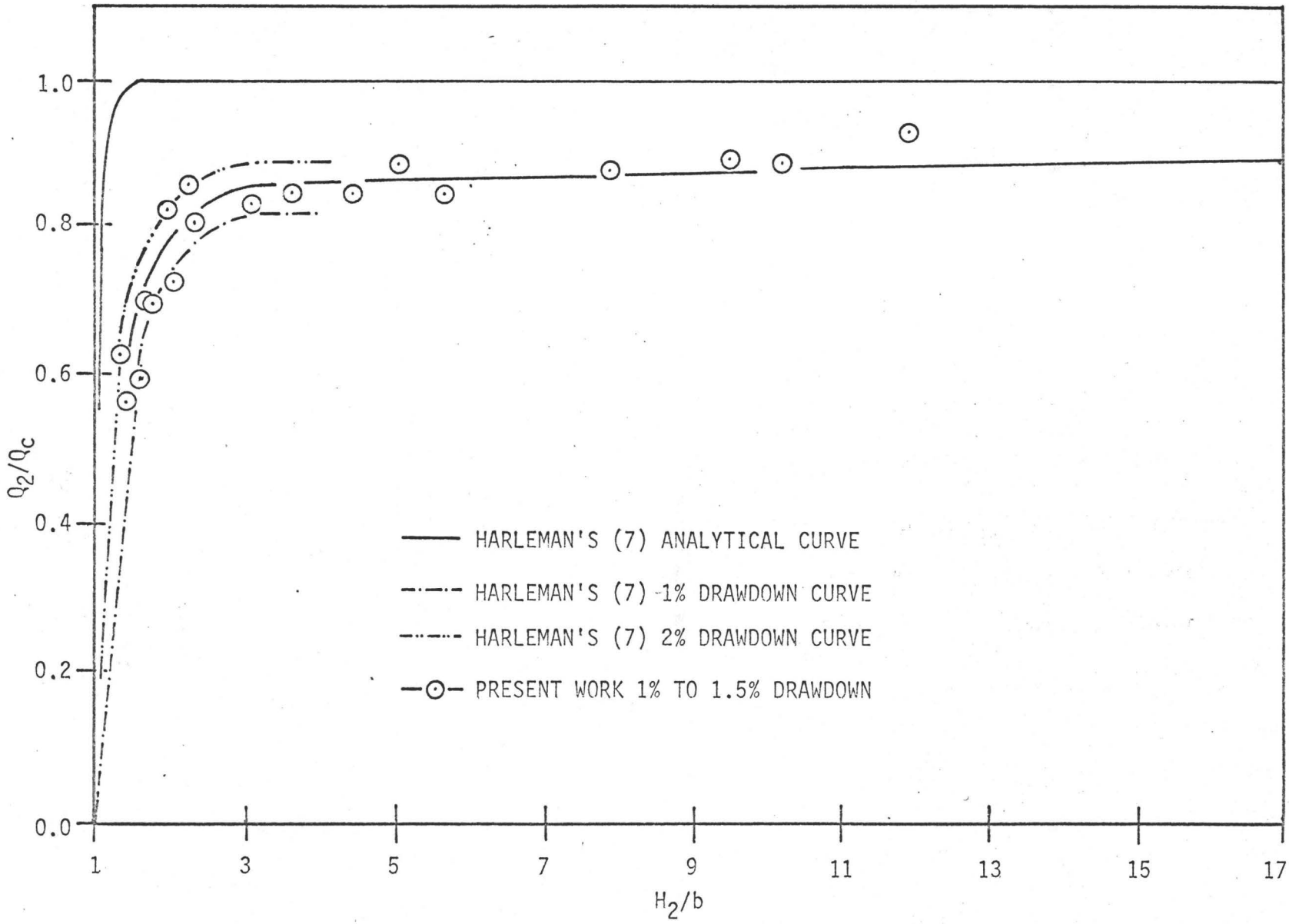

FIGURE 5.7: Q_2/Q_c vs. H_2/b

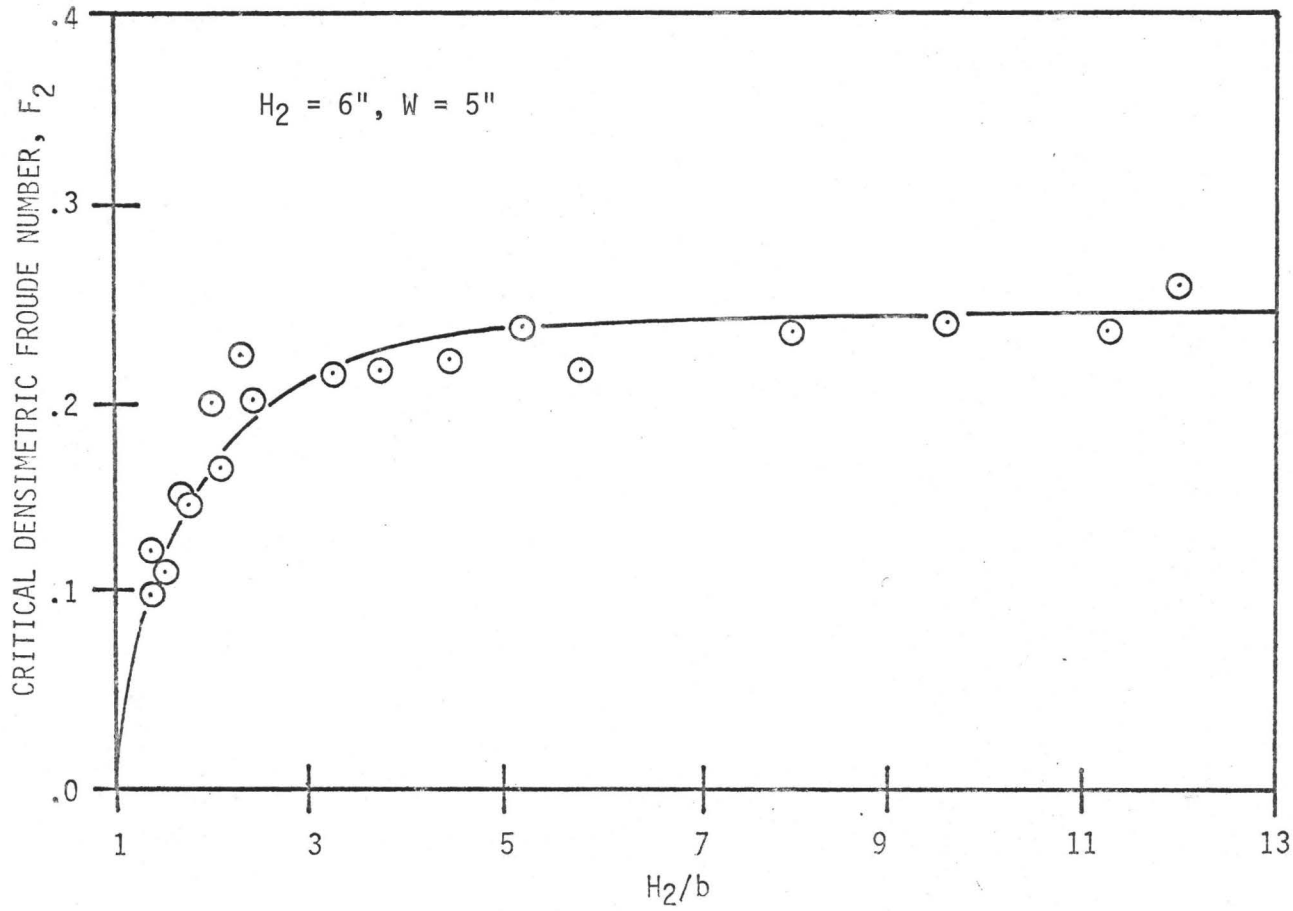

FIGURE 5.8: CRTICAL DENSIMETRIC FROUDE NUMBER, F_2, vs. H_2/b

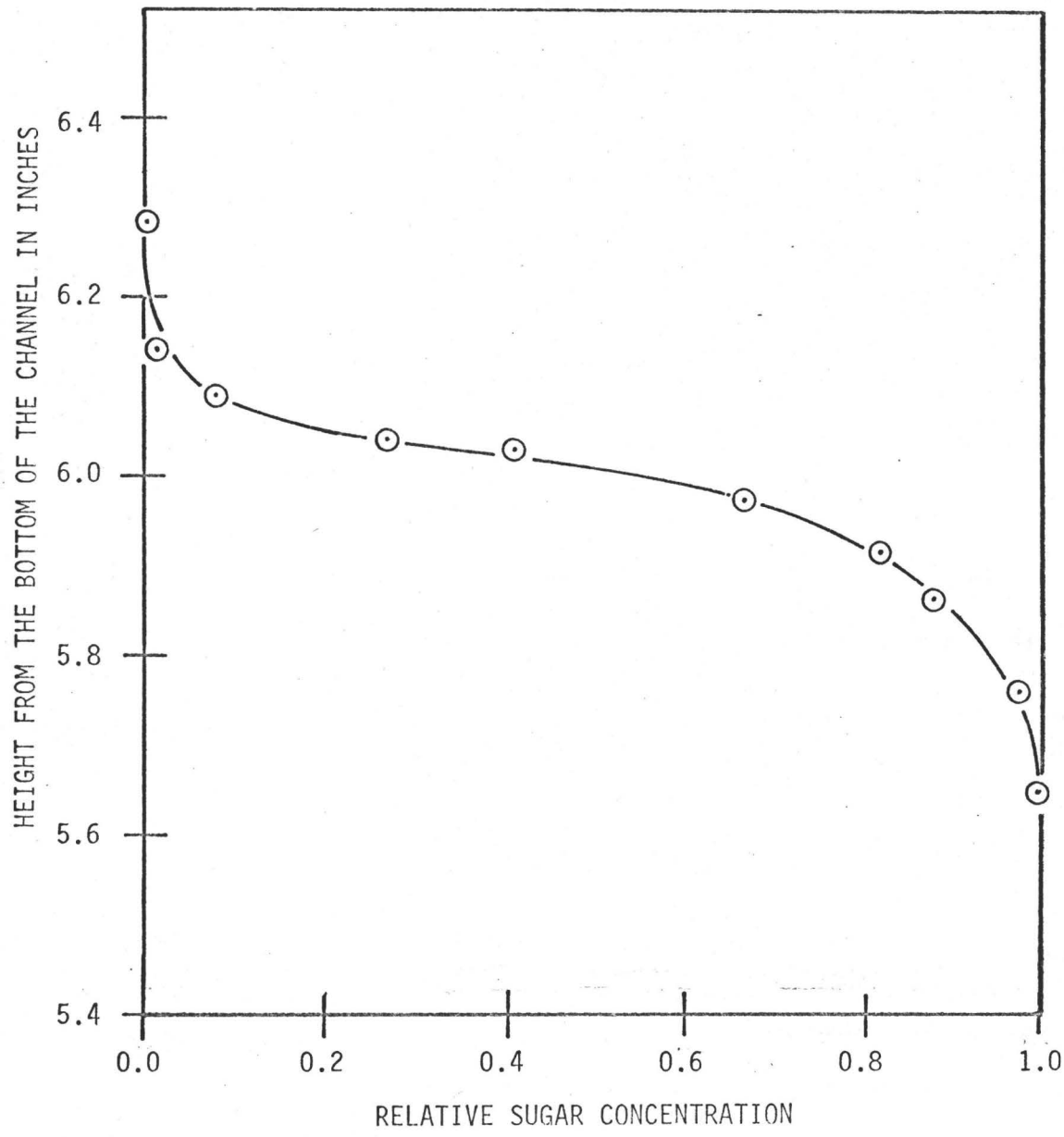

FIGURE 5.9: DENSITY VARIATION ACROSS INTERFACE

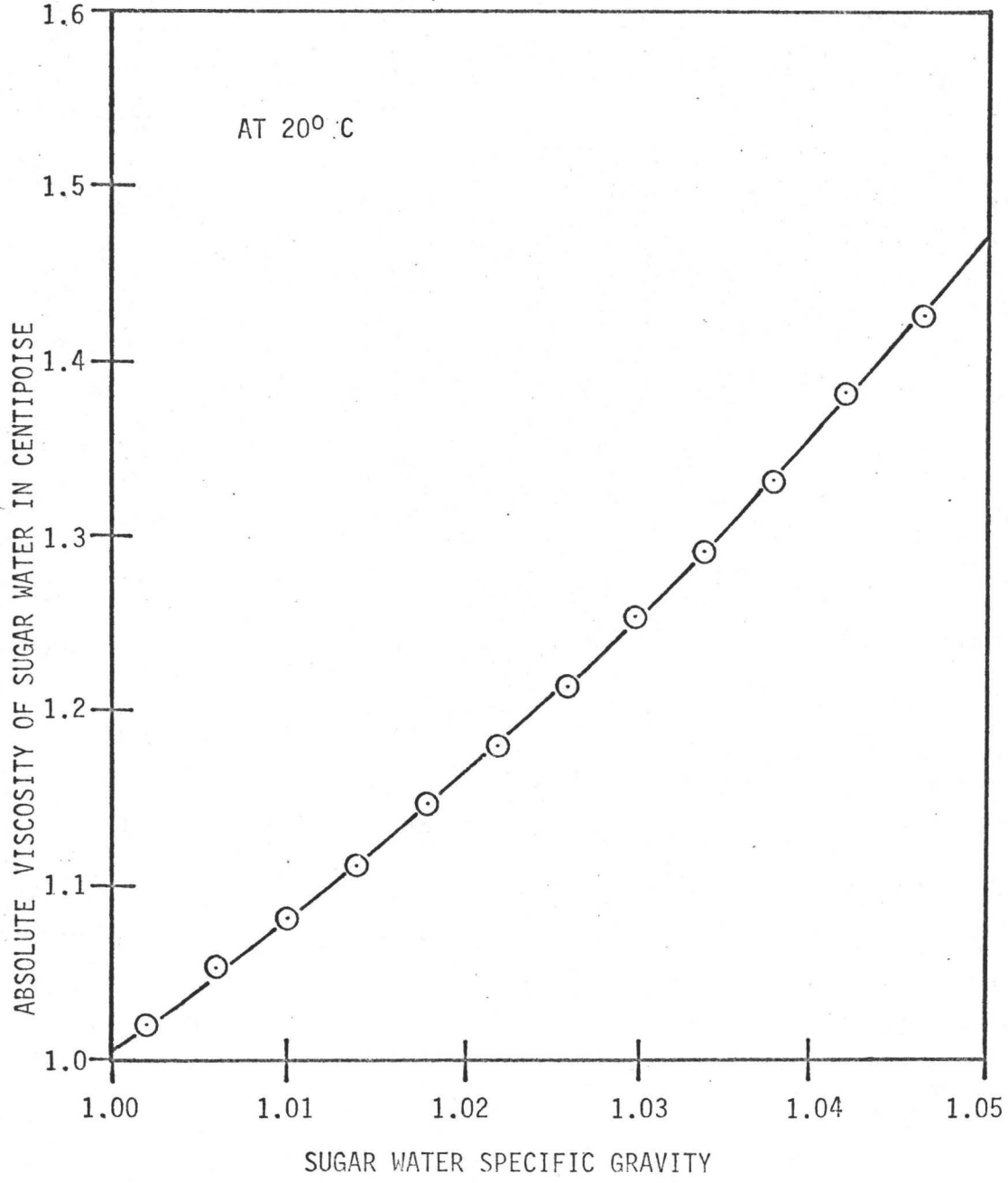

FIGURE 5.10: PLOT OF VISCOSITY vs. SPECIFIC GRAVITY OF SUGAR WATER, REFERENCES (19 AND 20).

TABLE NO. 5.1

$W=2"$, $H_2=6"$, $b=.312"$ Orifice #1 used

No.	Y in.	Q_2 $ft^3/sec.$	t sec.	S_2	S_1	V_2 ft/sec.	$ReyX10^{-3}$	e	F_2
1	2.9	.0177	31	1.0226	1.0009	.219	4.21	1.06	.129
2	4.3	.0214	28	1.0331	1.0009	.253	4.71	1.20	.127
3	2.7	.0170	32	1.0223	1.0009	.202	4.05	1.30	.121
4	4.3	.0213	23	1.0349	1.0008	.251	4.60	1.44	.119
5	2.95	.0177	33	1.0244	1.0006	.210	4.14	1.00	.119
6	5.7	.0245	21	1.0461	1.0009	.287	4.89	1.10	.119
7	1.9	.0143	36	1.0164	1.0008	.170	2.90	1.35	.117
8	2.1	.0152	35	1.0188	1.0009	.180	3.72	1.32	.116
9	4.55	.0220	30	1.0389	1.0009	.259	4.68	1.10	.114
10	6.0	.0251	26	1.0508	1.0009	.294	4.86	1.06	.113
11	6.5	.0263	20	1.0559	1.0009	.307	5.03	1.35	.112
12	3.75	.0200	32	1.0329	1.0008	.236	4.30	1.10	.111

TABLE NO. 5.2

W=3", H_2=6", b=.312" Orifice #2 used

NO.	Y in.	Q_2 $ft^3/sec.$	t sec.	S_2	S_1	V_2 ft/sec.	ReyX10^{-3}	e	F_2
1	2.5	.0362	25	1.0225	1.0006	.288	7.60	1.18	.230
2	2.25	.0345	31	1.0217	1.0007	.272	7.30	.980	.225
3	2.0	.0325	29	1.0192	1.0005	.257	7.02	1.10	.225
4	3.1	.0419	20	1.0324	1.0006	.330	8.22	1.25	.220
5	2.3	.0348	28	1.0222	1.0005	.273	7.30	1.36	.219
6	1.45	.0280	34	1.0151	1.0007	.222	6.22	1.23	.216
7	1.5	.0283	35	1.0153	1.0005	.224	6.29	1.06	.214
8	1.85	.0317	33	1.0196	1.0007	.251	6.80	1.00	.212
9	2.7	.0375	19	1.0279	1.0005	.293	7.54	1.49	.201
10	2.7	.0375	26	1.0283	1.0006	.295	7.56	1.00	.201
11	1.7	.0300	30	1.0184	1.0005	.237	6.50	1.16	.200
12	1.15	.0250	38	1.0133	1.0007	.198	5.61	1.10	.197
13	1.6	.0292	28	1.0180	1.0007	.231	6.43	1.28	.195
14	3.05	.0400	18	1.0333	1.0005	.314	7.76	1.47	.193

TABLE NO. 5.3

W=4", H_2=6", b=.312" Orifice #2 used

No.	Y in.	Q_2 $ft^3/sec.$	t sec.	S_2	S_1	V_2 ft/sec.	Rey$X10^{-3}$	e	F_2
1	5.0	.0508	22	1.0222	1.0007	.301	9.66	1.25	.268
2	4.8	.0498	26	1.0218	1.0007	.295	9.47	1.10	.262
3	4.3	.047	22	1.0193	1.0005	.276	9.01	1.37	.257
4	5.3	.0520	20	1.0243	1.0007	.308	9.72	1.35	.257
5	5.2	.0515	27	1.0241	1.0008	.305	9.66	1.01	.255
6	6.2	.0560	23	1.0284	1.0008	.331	10.1	1.09	.254
7	5.7	.0540	25	1.0263	1.0005	.319	9.98	1.04	.253
8	4.3	.0470	30	1.0202	1.0007	.279	9.07	1.00	.253
9	7.5	.0617	19	1.0341	1.0005	.363	10.7	1.20	.252
10	5.4	.0525	19	1.0252	1.0007	.310	9.74	1.41	.251
11	6.0	.0555	24	1.0281	1.0005	.328	10.1	1.05	.249
12	7.1	.0600	18	1.0332	1.0008	.354	10.5	1.30	.248
13	3.7	.0444	32	1.0187	1.0005	.264	8.66	.980	.243
14	3.7	.0440	30	1.0184	1.0005	.261	8.60	1.06	.242

TABLE NO. 5.4

W=5", H_2=6", b=.312" Orifice #2 used

No.	Y in.	Q_2 $ft^3/sec.$	t sec.	S_2	S_1	V_2 ft/sec.	$ReyX10^{-3}$	e	F_2
1	8.1	.0640	23	1.0218	1.0007	.302	11.0	1.20	.276
2	5.0	.0550	25	1.0163	1.0006	.261	9.90	1.27	.276
3	5.2	.0515	27	1.0145	1.0007	.244	9.37	1.26	.273
4	8.5	.0655	26	1.0228	1.0004	.310	11.2	1.03	.272
5	8.3	.0640	19	1.0222	1.0004	.303	11.0	1.44	.268
6	6.0	.0552	29	1.0167	1.0004	.262	9.90	1.37	.267
7	6.1	.0558	24	1.0172	1.0006	.265	9.97	1.30	.267
8	5.5	.0530	23	1.0158	1.0007	.252	9.55	1.43	.266
9	9.2	.0680	18	1.0258	1.0007	.321	11.4	1.44	.263
10	9.4	.0690	20	1.0252	1.0004	.327	11.6	1.30	.263
11	5.3	.0520	27	1.0152	1.0006	.247	9.37	1.24	.263
12	6.7	.0580	27	1.0188	1.0004	.275	10.2	1.12	.261
13	9.9	.0700	22	1.0277	1.0007	.331	12.0	1.14	.260

TABLE NO. 5.5

W=6", H_2=6", b=.312" Orifice #3 used

Np.	Y in.	Q_2 $ft^3/sec.$	t sec.	S_2	S_1	V_2 ft/sec.	$ReyX10^{-3}$	e	F_2
1	4.8	.086	17	1.0244	1.0003	.340	13.3	1.44	.299
2	3.35	.071	22	1.0174	1.0005	.281	11.6	1.34	.295
3	4.2	.080	25	1.0220	1.0003	.316	12.6	1.05	.292
4	3.5	.073	27	1.0189	1.0005	.289	11.8	1.06	.286
5	2.5	.0615	32	1.0138	1.0007	.244	10.3	1.06	.286
6	4.4	.082	22	1.0242	1.0007	.324	12.8	1.16	.284
7	3.1	.069	29	1.0172	1.0005	.273	11.3	1.05	.283
8	4.05	.079	19	1.0222	1.0003	.312	12.5	1.40	.282
9	4.35	.0815	22	1.0237	1.0003	.322	12.8	1.17	.282
10	3.2	.0700	24	1.0178	1.0005	.277	11.5	1.25	.281
11	2.65	.0635	31	1.0149	1.0007	.252	10.6	1.06	.281
12	4.1	.0790	24	1.0229	1.0007	.312	12.4	1.11	.279
13	2.8	.065	30	1.0160	1.0003	.258	10.7	1.07	.268
14	3.25	.071	28	1.0199	1.0003	.281	11.4	1.05	.258

TABLE NO. 5.6

$W=5"$, $H_2=6"$, Orifice #2 used

No.	H_2/b	Y in.	Q_2 $ft^3/sec.$	t sec.	S_2	S_1	Q_c $ft^3/sec.$	Q_2/Q_c	V_2 ft/sec.	Rey $X10^{-3}$	e	F_H	F_2
1	1.401	3.2	.0410	32	1.0258	1.0006	.0712	.568	.197	6.91	1.30	.51	.098
2	1.401	4.0	.0455	37	1.0253	1.0006	.0705	.637	.218	7.74	1.04	.57	.123
3	1.548	3.5	.0425	29	1.0242	1.0006	.0690	.608	.204	7.20	1.42	.64	.112
4	1.699	4.6	.0485	25	1.0230	1.0006	.0673	.711	.232	8.35	1.45	.875	.154
5	1.777	4.2	.0465	27	1.0221	1.0007	.0657	.699	.223	8.06	1.40	1.28	.147
6	1.979	5.6	.0535	28	1.0211	1.0007	.0640	.828	.257	9.34	1.16	1.26	.206
7	2.109	4.4	.0475	35	1.0207	1.0007	.0640	.737	.229	8.28	1.05	1.23	.165
8	2.285	5.9	.0550	28	1.0204	1.0007	.0630	.862	.264	9.53	1.10	1.63	.224
9	2.430	5.2	.0515	25	1.0200	1.0007	.0625	.815	.247	9.39	1.36	1.68	.200
10	3.254	5.4	.0528	23	1.0197	1.0003	.0627	.832	.253	9.28	1.49	2.59	.214
11	3.765	5.4	.0528	30	1.0194	1.0003	.0622	.850	.253	9.84	1.10	3.33	.213
12	4.571	5.5	.0530	24	1.0191	1.0003	.0617	.850	.254	9.40	1.40	4.53	.218
13	5.189	5.9	.0550	26	1.0187	1.0003	.0610	.893	.264	9.73	1.20	5.53	.240
14	5.810	5.2	.0515	30	1.0183	1.0003	.0604	.845	.247	9.17	1.10	6.46	.214
15	8.000	5.6	.0535	27	1.0181	1.0003	.0600	.880	.257	9.51	1.20	10.0	.234
16	9.600	4.7	.0490	25	1.0153	1.0008	.0486	.896	.235	8.88	1.40	14.5	.241
17	11.29	4.9	.0500	27	1.0164	1.0008	.0496	.880	.240	9.00	1.30	18.2	.234
18	12.00	6.0	.0555	24	1.0178	1.0003	.0595	.930	.266	9.88	1.30	20.4	.256

TABLE 5.7

Specific Gravity of Varsol (S_2) =.7840

W=2", H_2=4", b=.312" Orifice #2 used

No.	Y in.	Q_2 $ft^3/sec.$	S_1	V_2 ft/sec.	Rey $X10^{-3}$	F_2
1	4.0	.0455	1.0003	.819	19.3	.289
2	3.9	.0450	1.0003	.810	19.1	.283
3	3.8	.0442	1.0003	.795	18.7	.272
4	3.8	.0442	1.0003	.795	18.7	.272
5	3.8	.0442	1.0003	.795	18.7	.272
6	3.6	.0432	1.0003	.777	18.3	.260
7	3.5	.0428	1.0003	.770	18.2	.255

W=6", H_2=4", b=.312" Orifice #4 used

1	5.8	.185	1.0004	1.11	52.4	.531
2	5.8	.185	1.0004	1.11	52.4	.531
3	5.7	.184	1.0004	1.10	52.1	.525
4	5.6	.182	1.0004	1.09	51.4	.512
5	5.6	.182	1.0004	1.09	51.4	.512
6	5.6	.182	1.0004	1.09	51.4	.512
7	5.5	.180	1.0004	1.08	51.0	.502
8	5.4	.177	1.0004	1.06	50.0	.484

6. DISCUSSION

In the present experimental work definite wall effects were observed, which is in agreement with the observation made by Huber and Reid (2). Fig. 5.5 shows that as channel width increases the width effect decreases asymptotically,as one would expect, since the viscous boundary layer effects would be diminished. Even this limiting value of the densimetric Froude number was less than half of what was obtained by Reid (2) and far less than Huber's (1) analytical prediction. An attempt has been made to reinterpret Reid's (2) work as shown in the Appendix 3. It was also shown that using the 1% to 1.5% drawdown criteria, his results were closer to those obtained in this work.

The large discrepency between the experimental results and the analytical values could be explained by interfacial effects which were not taken into account in the analytical work by Huber (1). In fact the negative slope of the plot of F_1 against F_2, as shown in Fig.A3-1 was not observed in the results of this experimental work. This observation is further verified by the fact that in Fig.5.7 the ratio Q_2/Q_c, for the 2% drawdown case, was always greater than the 1% drawdown case, thus indicating that a larger flow rate for Q_2 was necessary to increase the quantity of the upper fluid flow rate , i.e. a positive slope for F_1 vs. F_2 curve. This

positive slope indicates that near the drawdown condition an increase in the velocity of the lower fluid layer would cause an increase in the velocity of the upper fluid. Thus indicating mutual viscous forces experienced by two fluids. All these above mentioned facts confirm the belief that interfacial viscous effects cannot be neglected in the case of flow towards a line sink. At higher velocities the slope of the curve increases very rapidly, a maximum value of F_2 is reached and then the curve follows the trend predicted by theory. Therefore,the entire flow region could be seen to be divided into two regions, a predominently viscous effects region and a predominently inertial effects region. As the difference between the velocities of the lower and the upper layers increases the interfacial viscous effects also increases, suggesting that the viscous effects would be maximum at the point of incipient drawdown.

The vortex pattern,as mentioned earlier,was due to the fact that two fluids used were real. The conditions assumed in Huber's (1) analytical work were altered because of presence of vortices.

A general agreement between the results obtained in the present work and Harleman's (7) experimental work was observed,as shown in Figs.5.6 and 5.7.

Even though Harleman's (7) theory is based wholly upon there being zero velocity upstream, and in the present work definite velocity existed far upstream, the present experimental work shows the same trend as that which was predicted by Harleman(7). The slight negative slope for a value of H_2/b greater than 2.5, as shown in Fig. 2.5 was not observed. Lack of data points left a doubt about the validity of the nature of the curve at the values of H_2/b greater than 2.5.

Interfacial mixing and wave breaking phenomena which was observed during experimental work was believed to cause a lowering of the value of the densimetric Froude number. Angelin and Flikested (8) and Streeter (18) have given the value of the parameter θ which is defined as,

$$\theta = \nu_2 g'/(V_2)^3$$

to be $(.18)^3$, at which interfacial waves would start breaking. Calculation of the velocity, based on this value of θ, indicates that interfacial waves start breaking at V_2=.11 ft/sec, ($\Delta S/S_2$ being assumed to be 0.023) which is less than the value of the velocity at which drawdown was observed. For this reason it was desirable to run tests with immiscible fluids and to establish quantitatively the effect of mixing and

interfacial waves breaking.

Tests using fresh water and varsol as the working fluids were run. The results, which are shown in Table 5.7, indicate that the value of the critical densimetric Froude number in this case is higher than that of sugar water and fresh water case. The results also indicate that the value of the critical densimetric Froude number in the case of 2" channel width is lower than that of a 6" channel width, thus indicating the presence of wall effects, which had already been established using sugar water and fresh water as working fluids.

7. CONCLUSIONS

1. It is deduced from the results that the critical densimetric Froude number is a function of the channel width. The wall effects being more pronounced at smaller widths.
2. Due to the breaking of the interfacial waves, which caused interfacial mixing, it was not possible to obtain a value of the densimetric Froude number closer to the analytical prediction by Huber (1). The apparent limiting value for the critical densimetric Froude number was found to be 0.28.
3. The experimental results indicate that the effect of the interfacial mixing is to lower the value of the critical densimetric Froude number in a two immiscible fluid system such as a fresh water and varsol.

8.REFERENCES

1. Huber, D.G.: "Irrotational Motion of Two Fluid Strata Towards a Line Sink", J.Eng. Mech. Div., Vol. 86, No. EM4, August 1960, pp.71-86.

2. Huber, D.G. and Reid, T.L.: "Experimental Study of Two Layered Flow Through a Sink", Proceedings ASCE, Vol.92, No. HY1, January, 1966, pp.31-41.

3. Harleman, D.R.F.,Morgan, R.L., Purple, R.A.: "Selective Withdrawal From a Vertically Stratified Fluid", Intern. Assoc. Hydr. Research, 8th Congress, August 1959.

4. Rouse. H., Davidian, J., : "Seven Exploratory Studies in Hydraulics" Proc. ASCE, Vol. 82, No. HY4, August 1956.

5. Harleman, D.R.F., Gooch, R.S., Ippen, A.T.: "Submerged Sluice Control of Stratified Flow", Proc. ASCE, Vol. 84, No. HY2, April 1958.

6. Elder, R.A., Dougherty, G.B., "Thermal Density Under Flow Diversion, Kingston Steam Plant", Proc. ASCE, Vol. 84, No. HY2, April 1958

7. Harleman, D.R.F., Elder, R.A.: "Withdrawal From Two Layered Stratified Flows", Proc. ASCE, HY4, July 1965.

8. Angelin, S.,Flikested; K., "An Investigation of Intake Arrangements for Cooling Water Supply Stratified Seawater", Intern. Assoc. Hydr. Research, 7th General Meeting 1957, pp. c-13-1 to c-13-10.

9. Bata, G.L.: "Recirculation of Cooling Water in Rivers and Canals", Proc. ASCE, Vol. 83, No.HY3, June 1958.

10. Macagno, E.O., Rouse H.,: "Interfacial Mixing in Stratified Flow", J.Eng. Mech. Div. ASCE, Vol. 87 October,1961.

11. Keulegan, G.H.: "Laminar Flow at the Interface of Two Liquids", Natl. Bur. Standards (U.S.), Circ. 32, 1944, pp.303.

12. Potter, O.E.: "Laminar Boundary Layer at the Interface of Co-current Parallel Streams", Quart. J. Mech. Appl. Math., August, 1957.

13. Wood, I.R.: "Horizontal Two Dimensional Density Current", Proc. ASCE, HY2, March, 1967.

14. Long, R.R.: "Velocity Concentrations in Stratified Fluids", Proc. ASCE, HY1, January, 1962.

15. Yih, C.S.: "On the Flow of Stratified Fluid", 3rd U.S. Natl. Congr. Appl. Mech., 1958

16. Yih, C.S.: "On Stratified Flows in a Gravitational Field", Tellus, Vol. 9, No. 2, 1957.

17. Debler, W.R.: "Stratified Flow into a Line Sink", Proc. ASCE, Vol. 85, No. EM3, July, 1959.

18. Streeter, V.L.: "Handbook of Fluid Dynamics", McGraw Hill Company, 1961, Chapter 26.

19. Hodgman, C.D., West R.C. and Selby, S.M.,: "Handbook of Physics and Chemistry", 42nd Edition, page 2211

20. Hodgman, C.D.; "Handbook of Chemistry and Physics", 29th Edition, page 1590

21 Khafagi, A., Hammad, S.: "Velocity and Pressure Distribution in Curved Stream Line Flow", Water and Water Engineering, March 1954

APPENDICES

APPENDIX-1

ORIFICES

a. Orifice Design:

In order that the flow rate could be measured accurately several orifices were used in conjunction with each of the channel widths.

By knowing an approximate value of the Froude number at the incipient drawdown point and the density difference, the velocity could be calculated from following equation,

$$F_2 = (V_2)^2 / (H_2.g.(\Delta S/S_2)) \text{ --------(A.1.1)}$$

For a certain channel width an approximate maximum flow rate could be calculated, assuming value for ΔS and F_2. The following formula was used for the orifice meter,

$$Q = K A (2g (p_1-p_2)/\gamma_w)^{\frac{1}{2}} \text{ ----------(A.1.2)}$$

where:

p_1-p_2 = Pressure difference across the orifice (lbf/ft^2)

Q = Volume flow rate ($ft^3/sec.$)

K = Orifice constant

A = Orifice area (ft^2)

γ_w = Weight density of water (lbf/ft^3)

$\gamma_{Hg.}$ = Weight density of mercury (lbf/ft^3)

Now the difference between the levels of the mercury in the two limbs of the manometer is twice that for one of the limb above the null condition, therefore we may write,

$$p_1 - p_2 = \gamma_{Hg.}(2Y) \text{ ----------(A.1.3)}$$

$$Q = K A (2g \gamma_{Hg.} 2Y / \gamma_w)^{\frac{1}{2}} \text{ -------(A.1.4)}$$

$$A = \pi d^2 / 4 \text{ ----------(A.1.5)}$$

where,

d = Orifice diameter, (ft)

giving,

$$d = \left[(4Q/\pi K) \left(\frac{\gamma_w}{\gamma_{Hg.} 4 g Y} \right)^{\frac{1}{2}} \right]^{\frac{1}{2}} \text{------(A.1.6)}$$

Assuming K to be .62 and $\gamma_{Hg.}/\gamma_w$ to be 13.6 and knowing Q and other parameters in eqn. A.1.6 the orifice diameter could be calculated.

b. Orifice Calibration:

The four orifices, that were used, were calibrated prior to use, using standard calibration tank.

APPENDIX-2

NOTE ON THE ANALYTICAL SOLUTION TO THE PROBLEM AS PROPOSED BY HUBER (1)

Huber (1), in his analysis, applied Bernoulli equation between two points at the interface, one point being upstream and other near the sink, see Fig. 1.1. The following two relations can be written,

$$p_{1\infty} + \rho_1 V_{1\infty}^2/2 + \gamma_1 y_\infty = p_{1A} + \rho_1 V_{1A}^2/2 + \gamma_1 y_A \text{----(A.2.1)}$$

$$p_{2\infty} + \rho_2 V_{2\infty}^2/2 + \gamma_2 y_\infty = p_{2A} + \rho_2 V_{2A}^2/2 + \gamma_2 y_A \text{----(A.2.2)}$$

where p is pressure, ρ is mass density, γ is specific weight, y is vertical distance measured from the horizontal line representing the interface. The subscript ∞ refers to the upstream point and A refers to a point near the sink. Upon subtraction and introducing the relationships $p_{1\infty} = p_{2\infty}$, $p_{1A} = p_{2A}$ and $y_\infty = 0$ the equation for the interface becomes,

$$(\rho_1/2)(V_{1A}^2 - V_{1\infty}^2) - (\rho_2/2)(V_{2A}^2 - V_{2\infty}^2) = y_A \cdot \Delta\gamma \text{---(A.2.3)}$$

where,

$$\Delta\gamma = \gamma_2 - \gamma_1$$

Upon using the eqn. A.2.3 as a boundary condition for a potential flow problem, it is obvious that the possibility of a rigorous

mathematical determination of the stream function in each potential field becomes difficult. Since it is difficult to obtain a rigorous mathematical solution, an approximate numerical analysis was employed to solve the problem.

The method used for the solution was a relaxation procedure which necessitated an initial assumption as to the form of the interfacial shape and secondly an estimation of the stream function ψ throughout the two potential fields. By relaxation technique the assumed values of ψ were altered until they were corrected at every point for the assumed boundary conditions. Velocities were calculated at a number of points along the interface and the interfacial equation A.2.3 was checked to determine if the boundary condition was satisfied. By the use of constants in the equation it was possible to calculate the two velocities at every point and thus the densimetric Froude number, once the correct interfacial shape was obtained. The interfacial angle was also measured and plotted against the densimetric Froude number.

APPENDIX-3

REINTERPRETATION OF REID'S (2) WORK

Reid's (2) work basically verified Huber's (1) analytical work. The experimental points, Fig. A 3-1, deviate from his suggested curve as F_1 decreased to the values less than F_1=.2. If these points are plotted with an enlarged scale, Fig. A 3-3, this deviation becomes apparent. Near the point of incipient drawdown the value for densimetric Froude number varied appreciably. When $(F_1)^{\frac{1}{2}}$ is plotted against $(F_2)^{\frac{1}{2}}$, as shown in Fig. A 3-4, the point corresponding to F_2 = .756 assumes a considerably higher value of $(F_1)^{\frac{1}{2}}$, making its acceptance as a drawdown point doubtful. The percentage volume flow rate of the upper fluid was computed to be as high as 10% at F_2= .756.

An alternative curve passing through Reid's (2) points was drawn, Fig.A 3-3 and Fig.A 3-4. This alternative curve is in agreement with Harleman's (7) experimental curve.

The changing nature of the curve could be explained by the relative influence of the velocity. Near the drawdown condition, when the velocity difference between the two layers is high, the viscous effects are dominant. At high densimetric Froude numbers, the two fluids flow at nearly the same velocity, therefore, the trend of curve is essentially

the same as was predicted by Huber's (1) inviscid theory.

It should be noticed that there are some typographical errors in Table 5.1 of Reid's (2) thesis. The scale reading and the volume of the sugar solution collected in the tank do not correspond to each other from run 41 to 46. However, these errors do not appear in his graphs.

In Fig. A 3-2 no experimental measurements are given for the point corresponding to $H_2/b=6$. In fact this was the only point which lies in the region where the curve sharply changes its direction.

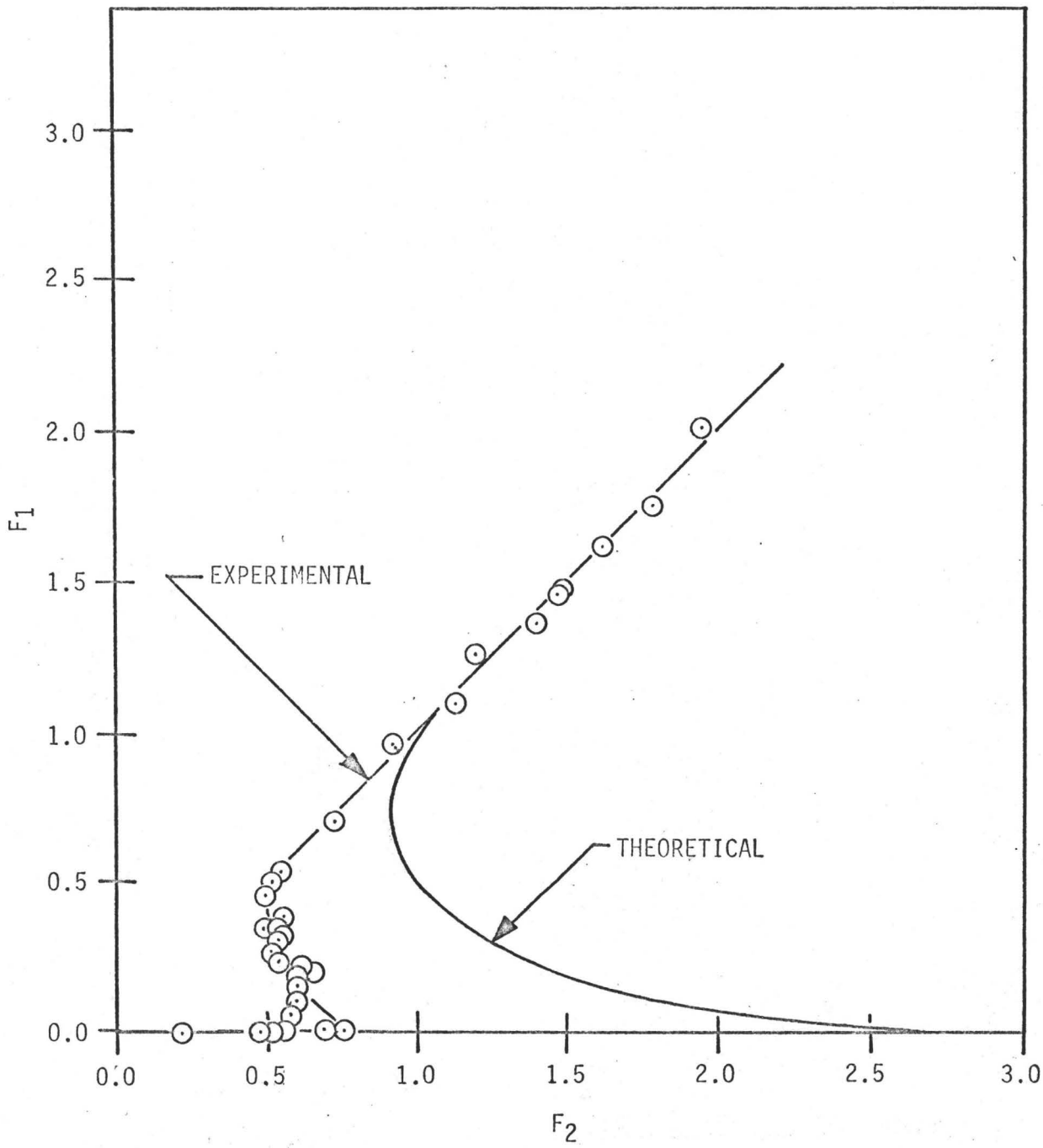

FIGURE A 3-1: ANALYTICAL AND EXPERIMENTAL RESULTS OF HUBER (1) AND REID (2)

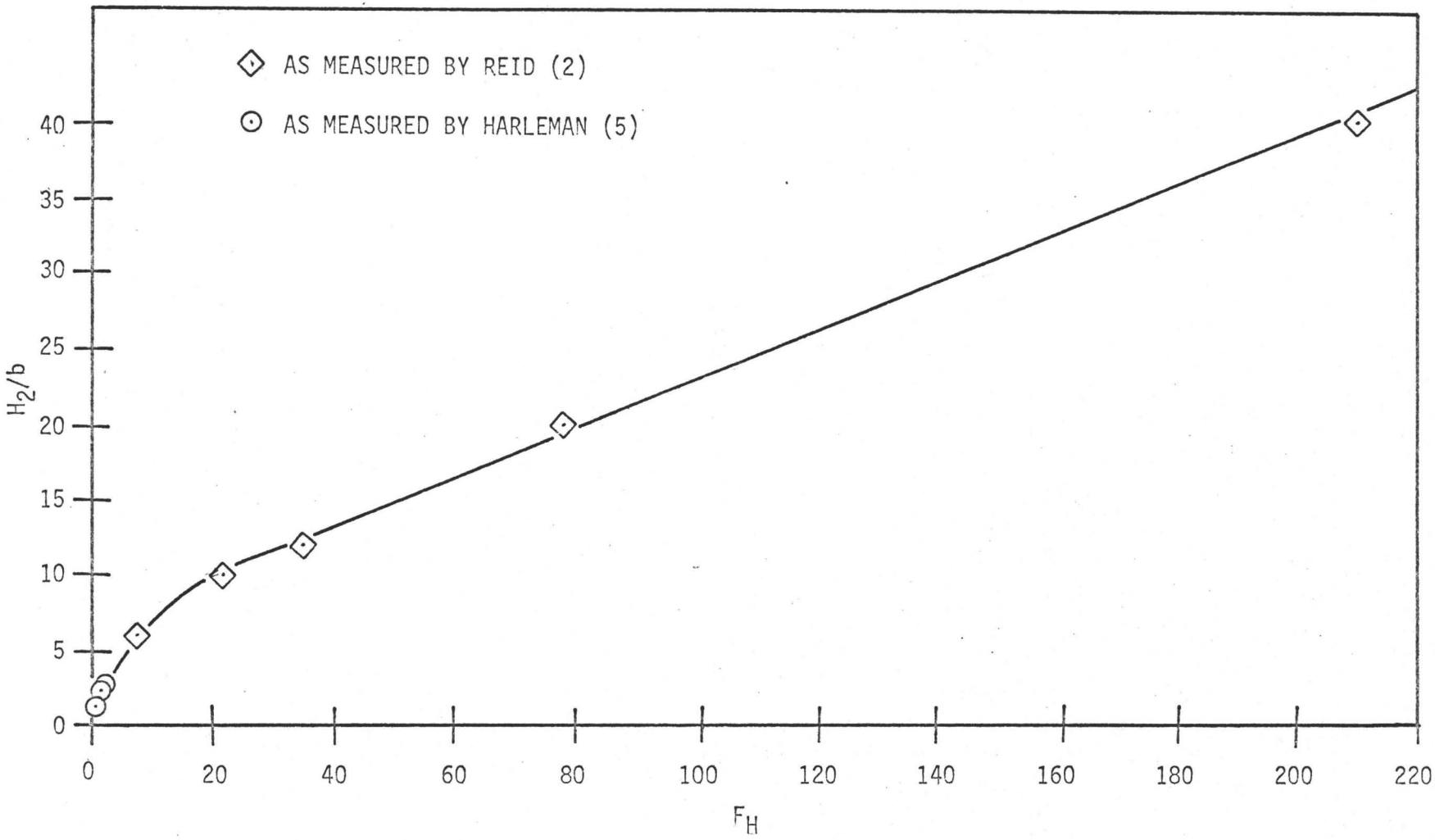

FIGURE A 3-2: H_2/b vs. CRITICAL DENSIMETRIC FROUDE NUMBER, F_H

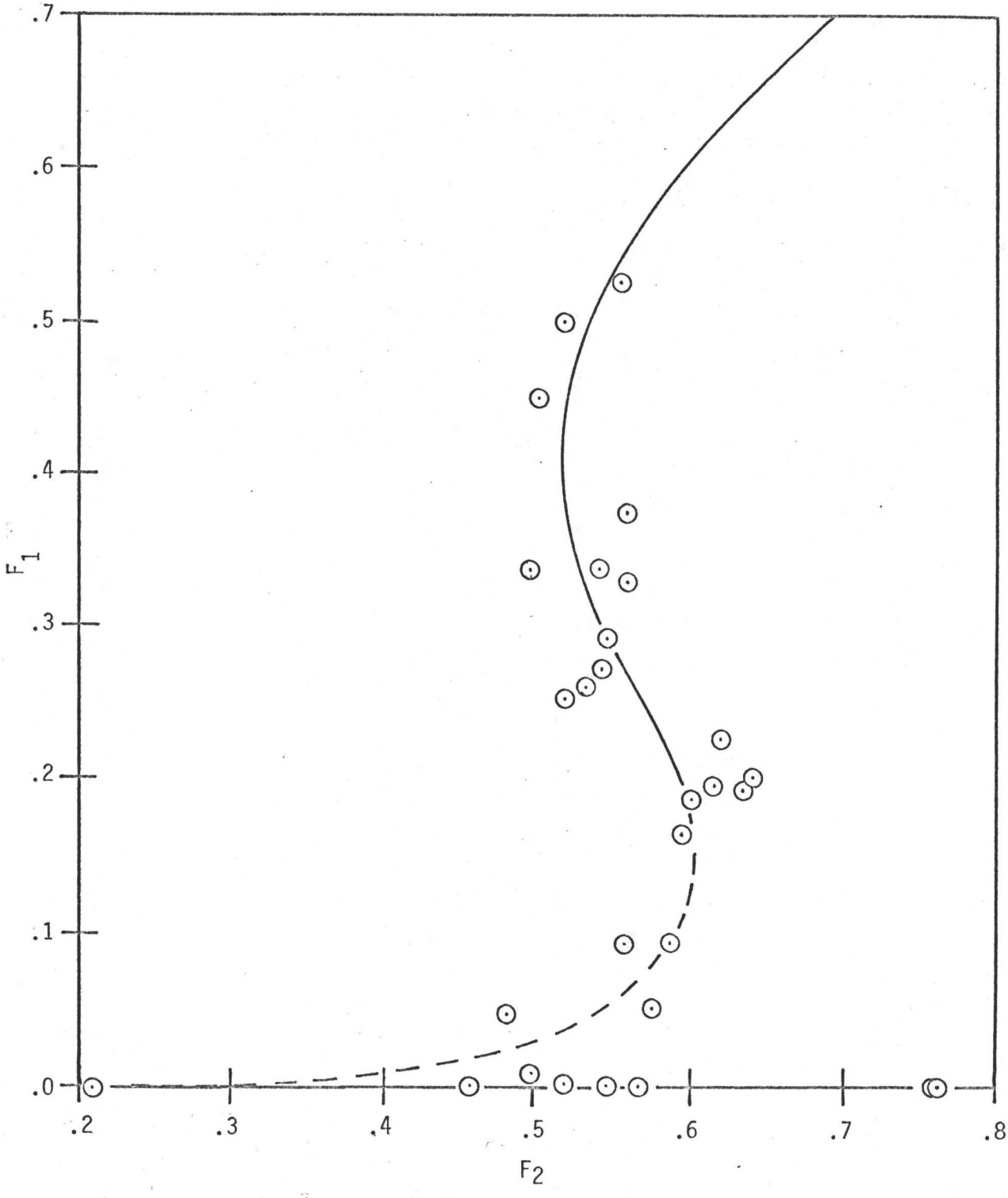

FIGURE A 3-3: REID'S EXPERIMENTAL RESULTS, F_1 vs. F_2

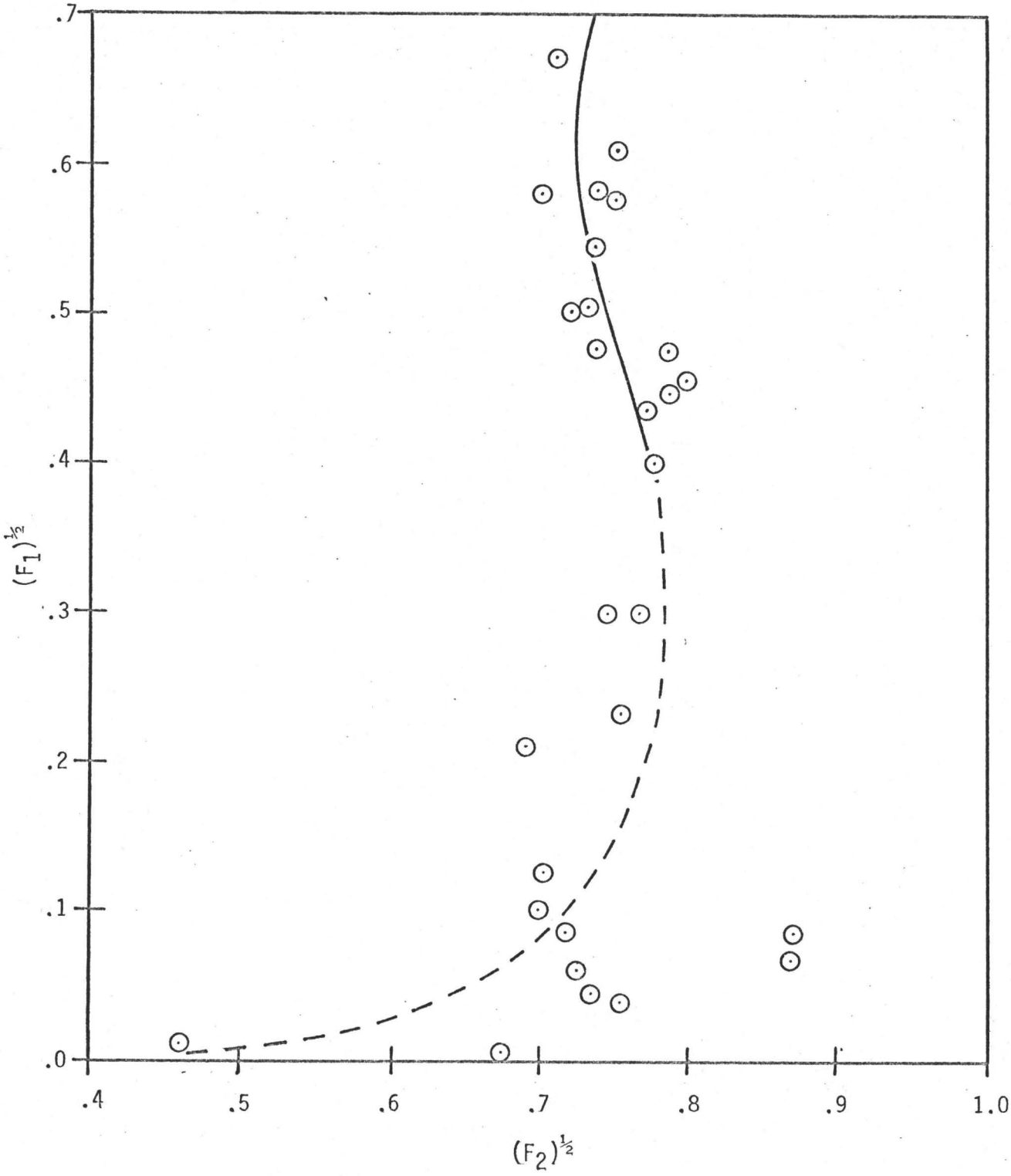

FIGURE A 3-4: REID'S EXPERIMENTAL RESULTS, $(F_1)^{\frac{1}{2}}$ vs. $(F_2)^{\frac{1}{2}}$

APPENDIX-4

DEFINITION OF THE DENSIMETRIC FROUDE NUMBERS USED

The densimetric Froude number used in this thesis is defined as follows,

$$F_2 = (V_2)^2 / (H_2.g.(\Delta S/S_2))\text{-------(A.4.1)}$$

The densimetric Froude number, as defined by Harleman, and used in this thesis is as follows,

$$F_H = (Q_2/W.b) / (g (\Delta S/S_2) b)^{\frac{1}{2}} \text{ -----(A.4.2)}$$

A relation between the two densimetric Froude number could be obtained by rearranging various terms.

$$F_H^2 = (Q_2/W.H_2)^2/[(b/H_2)^3.H_2.g.(\Delta S/S_2)]\text{-(A.4.3)}$$

or

$$F_H^2 = F_2 (H_2/b)^3 \text{ ----------(A.4.3)}$$

APPENDIX-5

ERROR ANALYSIS

i. Error in Densimetric Froude Number 'F_2':

The densimetric Froude number in present work is defined as follows,

$$F_2 = \frac{V_2^2}{H_2\, g\, (\Delta S/S_2)} \qquad \text{----------(A.5.1)}$$

Differentiating and dividing both sides by F_2 we get,

$$\frac{dF_2}{F_2} = 2.\frac{dV_2}{V_2} - \frac{dH_2}{H_2} + \frac{dS_2}{S_2} - \frac{d\Delta S}{\Delta S} - \frac{dg}{g} \qquad \text{----------(A.5.2)}$$

The velocity V_2 was calculated from the volume flow rate as shown below,

$$V_2 = Q_2 / (H_2.W) \qquad \text{---------- (A.5.3)}$$

Differentiating and dividing both sides by V_2 we get,

$$\frac{dV_2}{V_2} = \frac{dQ_2}{Q_2} - \frac{dH_2}{H_2} - \frac{dW}{W} \qquad \text{----------(A.5.4)}$$

The volume flow rate (Q_2) was measured using orifice plates which had been calibrated by using a measuring tank. The volume flow rate (Q_2) was calculated by measuring the initial and final level of water in the tank called X_1 and X_2 respectively and time taken (T) to fill it, that is,

$$Q_2 = c\,(X_2 - X_1) / T \quad \text{---------- (A.5.5)}$$

where c is calibration constant of measuring tank in $ft^3/in.$

Differentiating and dividing both sides of equation A.5.5 by Q_2 we get,

$$\frac{dQ_2}{Q_2} = \frac{dc}{c} + \frac{dX_2}{(X_2-X_1)} - \frac{dX_1}{(X_2-X_1)} - \frac{dT}{T} \quad \text{---------- (A.5.6)}$$

Equations A.5.2, A.5.4 and A.5.6 are combined to give following,

$$\frac{dF_2}{F_2} = \left[\frac{dX_2}{(X_2-X_1)} - \frac{dX_1}{(X_2-X_1)} + \frac{dc}{c} - \frac{dT}{T} - \frac{dH_2}{H_2} - \frac{dW}{W}\right].2$$

$$- \frac{dH_2}{H_2} + \frac{dS_2}{S_2} - \frac{d\Delta S}{\Delta S} - \frac{dg}{g} \quad \text{----------(A.5.7)}$$

ii. Error in Percentage Drawdown 'e' :

By knowing the volume flow rate of the upper and lower fluids, the percentage drawdown of the upper layer was calculated from the following equation,

$$e = (Q_1/Q_2) \times 100 \quad \text{----------(A.5.8)}$$

therefore,

$$\frac{de}{e} = \frac{dQ_1}{Q_1} - \frac{dQ_2}{Q_2} \quad \text{----------(A.5.9)}$$

Similarly,

$$\frac{dQ_1}{Q_1} = \frac{d\Delta H_2}{\Delta H_2} + \frac{dW}{W} + \frac{dL}{L} - \frac{dt}{t} \qquad \text{---------- (A.5.11)}$$

From equations A.5.6, A.5.9 and A.5.11, we get,

$$\frac{de}{e} = \frac{d\Delta H_2}{\Delta H_2} + \frac{dW}{W} + \frac{dL}{L} - \frac{dt}{t} - \frac{dc}{c} - \frac{dX_2}{(X_2-X_1)} + \frac{dX_1}{(X_2-X_1)} + \frac{dT}{T} \qquad \text{----------(A.5.12)}$$

iii. Error in the Densimetric Froude Number 'F_H' :

The densimetric Froude number as defined and used by Harleman (5) is as follows,

$$F_H = \frac{(Q_2 / W.b)}{(g.(\Delta S/S_2).b)^{\frac{1}{2}}} \qquad \text{----------(A.5.13)}$$

therefore,

$$\frac{dF_H}{F_H} = \frac{dX_2}{(X_2-X_1)} - \frac{dX_1}{(X_2-X_1)} + \frac{dc}{c} - \frac{dT}{T} - \frac{dW}{W} - \frac{db}{b} + \tfrac{1}{2}\left[\frac{dS_2}{S_2} - \frac{dg}{g} - \frac{db}{b} - \frac{d\Delta S}{\Delta S}\right] \qquad \text{------(A.5.14)}$$

iv. Error in the Ratio 'H_2/b':

$$\frac{d(\ H_2/b\ )}{H_2/b} = \frac{dH_2}{H_2} - \frac{db}{b} \qquad \text{----------(A.5.15)}$$

v. Error in the Ratio 'Q_2/Q_c':

$$\frac{d(\ Q_2/Q_c\ )}{Q_2/Q_c} = \frac{dQ_2}{Q_2} - \frac{dQ_c}{Q_c} \qquad \text{----------(A.5.16)}$$

The critical discharge rate as derived by Harleman (7) is given by,

$$Q_c = W\ (\ g.(\ \Delta S/S_2).(\ \frac{2}{3}\ H_2)^3\ )^{\frac{1}{2}} \qquad \text{---------(A.5.17)}$$

therefore,

$$\frac{dQ_c}{Q_c} = \frac{dW}{W} + \tfrac{1}{2}.\left[\frac{dg}{g} + \frac{d\,\Delta S}{\Delta S} - \frac{dS_2}{S_2} + 3\,\frac{dH_2}{H_2}\right] \qquad \text{(A.5.18)}$$

To sum up, the estimated errors in various measured quantities are tabulated below,

	Quantity	Estimated Maximum Error
i.	$dX_2/(X_2-X_1)$	±.62%
ii.	$dX_1/(X_2-X_1)$	±.62%
iii.	dc/c	±.24%
iv.	dT/T	±.1%
v.	dH_2/H_2	±.52%
vi.	dW/W (maximum in case of W=2")	±1.56%
vii.	dS_2/S_2	±.01%

viii.	d $\Delta S/ \Delta S$ (maximum when S_2= .014)	±.71%
ix	db/b (calculated at H_2/b=3)	±1.56%
x.	dL/L	±.13%
xi.	dt/t	± 4%
xii.	d $\Delta H_2/ \Delta H_2$	± 25%

Total maximum errors in various quantities would be as follows,

Quantity	Estimated Total Maximum Error
F_2	±8.56%
e	±32.27%
F_H	±5.84%
H_2/b	±2.08%
Q_2/Q_c	±4.28%

Because of the large percentage error in e, the maximum and minimum drawdown percentages would be of the order of 2% and .7% respectively, instead of 1.5% and 1%. It could be noticed that even in the worst case uncertainity in e would not be more than 0.5%.

APPENDIX-6

OTHER METHODS WHICH WERE INVESTIGATED TO DETERMINE DRAWDOWN

Various methods to determine drawdown were attempted before the final method was chosen.

A hydrogen bubble technique was tried. Four wires were put across the channel near the sink. Insulations of the wires were removed at several places and the wires were adjusted in such a way so that exposed portions lie near the liquid-liquid interface. The D.C. current was passed through the wires and hydrogen bubbles were formed. The path of hydrogen bubbles were expected to indicate the velocity profile in the upper fluid. The bouyancy effect predominated in the low velocity regions and therefore, the hydrogen bubble technique was of little value when used for the upper fluid, and consequently was not employed.

A second technique, which was tried, was that of injecting dye at different locations in the upper fluid layer. It was observed that the fluid particles of the upper fluid layer which were adjacent to the liquid-liquid interface were found to be moving along with the lower fluid, even though no drawdown had occured, thus establishing a vortex in the upper fluid layer. After repeating the procedure at different densimetric Froude numbers no definite change in the behaviour of dye movement was observed near the drawdown.

APPENDIX-7

VISCOUS FLOW AT THE INTERFACE OF TWO FLUIDS

Keulegan's (11) work is of particular interest as it gives an insight into the flow at the interface between two viscous fluids. The two fluids he considered were of different density and viscosity. The Prandtl's boundary layer equation for the two-dimensional flow of an incompressible fluid can be written as follows,

$$u \frac{\partial u}{\partial x} + v \frac{\partial u}{\partial y} = \nu \frac{\partial^2 u}{\partial y^2} - \frac{1}{\rho} \frac{\partial p}{\partial x} \quad \text{-------- (A.7.1)}$$

The laws of hydrostatic pressure and continuity can be expressed as,

$$\frac{1}{\rho} \frac{\partial p}{\partial y} + g = 0 \quad \text{----------(A.7.2)}$$

$$\frac{\partial u}{\partial x} + \frac{\partial v}{\partial y} = 0 \quad \text{----------(A.7.3)}$$

where u and v are the components of velocity in the x and y direction respectively and p is the hydrostatic pressure. Adopting a characteristic length δ which is to be regarded as a function of x only, the two dimensionless variables are defined as,

$$\eta \doteq n.y / \delta \quad \text{---------- (A.7.4)}$$

and,

$$H(\eta) = -\psi / U.\delta \quad \text{----------(A.7.5)}$$

where ψ is stream function, U is free stream velocity and η is dimensionless numerical constant to be specified later. Introducing new variables, η and $H\eta$, and noting that $\frac{\partial p}{\partial x} = 0$, eqn. A.7.1 becomes,

$$U \frac{\partial \delta}{\partial x} H \frac{\partial^2 H}{\partial \eta^2} + \eta \frac{\nu}{\delta} \frac{d^3 H}{d\eta^3} = 0 \quad \text{----------(A.7.6)}$$

Thus if δ is selected in such a way so as to satisfy the relation,

$$\delta^2 = 2 n (\nu x/U) \quad \text{----------(A.7.7)}$$

then from eqn. A.7.6 we have,

$$\frac{d^3 H}{d\eta^3} + H \frac{d^2 H}{d\eta^2} = 0 \quad \text{----------(A.7.8)}$$

which is Blausius equation for the laminar boundary layer when the pressure is independent of x. Now,

$$u = -\frac{\partial \psi}{\partial y} = n U \frac{dH}{d\eta} \quad \text{----------(A.7.9)}$$

hence if we specify that $dH/d\eta = 1$ for large values of η, and this is a boundary condition for the upper fluid, we must then take $n=1$.

Summarizing we have for the upper fluid,

$$\frac{d^3 H}{d\eta^3} + H \frac{d^2 H}{d\eta^2} = 0 \quad \text{----------(A.7.10)}$$

where,

$$H = -\psi / U.\delta ; \quad \eta = y/\delta$$

and,

$$\delta = (2\nu x / U)^{\frac{1}{2}}$$

Similarly for the lower fluid we have,

$$\frac{d^3H'}{d\eta'^3} + H' \frac{d^2H'}{d\eta'^2} = 0 \qquad \text{----------(A.7.11)}$$

where,

$$H' = -\psi' / U.\delta' ; \quad \eta' = y'/\delta'$$

and,

$$\delta' = (2\nu' x / U)^{\frac{1}{2}}$$

Six boundary conditions are required to solve the equations A.7.10 and A.7.11 simultaneously. In the upper liquid u equals U for $y=\infty$, and in the lower liquid u' vanishes for $y'=\infty$, Accordingly,

$$\frac{dH}{d\eta} = 1 \qquad \text{when} \quad \eta = \infty \qquad \text{------(A.7.12)}$$

$$\frac{dH'}{d\eta'} = 0 \qquad \text{when} \quad \eta' = \infty \qquad \text{-------(A.7.13)}$$

If interface is to remain horizontal, we must have,

$$H = 0 \qquad \text{at} \quad \eta = 0 \qquad \text{---------(A.7.14)}$$

$$H' = 0 \qquad \text{at} \quad \eta' = 0 \qquad \text{---------(A.7.15)}$$

The velocities are continuous at the interface, hence,

$$\frac{dH}{d\eta} = \frac{dH'}{d\eta'} \qquad \text{when } \eta = \eta' = 0 \text{ ---- (A.7.16)}$$

Again shearing forces are continuous at the interface hence ,

$$\mu \frac{\partial u}{\partial y} = -\mu' \frac{\partial u'}{\partial y'} \qquad \text{when } y = y' = 0$$

$$\frac{d^2H}{d\eta^2} = -r \frac{d^2H'}{d\eta'^2} \qquad \text{when } \eta = \eta' = 0$$

where ,

$$r^2 = \mu'\rho' / \mu\rho$$

Keulegan (11) adopted method of approximation in order to solve equations A.7.10 and A.7.11. The interfacial laminar velocity distribution for the case $r^2=1$, as obtained by Keulegan, (11), is shown in Fig. A.7-1.

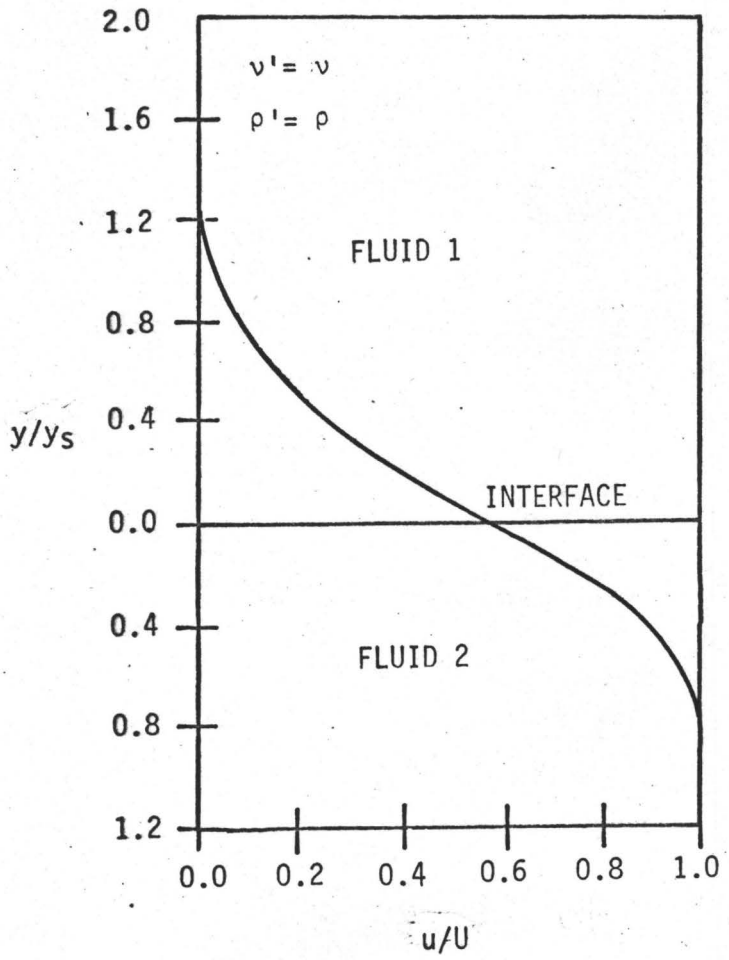

FIGURE A 7-1: INTERFACIAL LAMINAR VELOCITY DISTRIBUTION

APPENDIX-8

ESTIMATION OF THE WALL EFFECT ON THE DENSIMETRIC FROUDE NUMBER

There will be boundary layers formed at the walls of the channel. Consequently the free stream velocity in the channel would be higher than average velocity, which is calculated on the basis of bulk volume flow.

Let us say at certain distance X from the point of starting of boundary layer formation, it is desired to find difference in the calculated densimetric Froude number and the existing free stream densimetric Froude number.

If V_c be the free stream velocity then laminar boundary layer thickness δ at distance X could be written as,

$$\delta = 5.6 \left(\nu X / V_c \right)^{\frac{1}{2}} \text{ ----------(A.8.1)}$$

where,

δ is boundary layer thickness

ν is kinemetic viscosity

The equation A.8.1 was based on Blasius solution for laminar boundary layer case.

The volume flow rate in the boundary layer (q_1) can be obtained by integrating velocity distribution in the layer.

$$q_1 = \int_0^{\delta} u \, dy \text{ ----------(A.8.2)}$$

At the interface the volume flow rate in the layer (q_2) again can be obtained by integrating the velocity distribution.

$$q_2 = \int_0^{y_s} u \, dy \qquad \text{----------(A.8.3)}$$

From Keulegan's work (11) y_s could be written as,

$$y_s = 4.75 \, (\nu \, x / V_c)^{\frac{1}{2}}$$

where ,

x is the distance from the point where two fluids come togather

In Fig. A 8-1 the boundary layers thickness at the bottom and at sides are assumed to be of the same.

Now the total volume flow rate can be written as,

$$Q_T = V_c(W-2\delta)(H_2-\delta-y_s)+2H_2 q_1 + q_1(W-2\delta) + q_2(W-2\delta) \qquad \text{----------(A.8.4)}$$

The total volume flow rate can also be expressed as,

$$Q_T = V_2.W.H_2 \qquad \text{----------(A.8.5)}$$

therefore,

$$V_2.W.H_2 = V_c(W-2\delta)(H_2-\delta-y_s) + 2 H_2 q_1 + q_1(W-2\delta) + q_2(W-2\delta) \qquad \text{----------(A.8.6)}$$

and q_1 and q_2 can further be expressed and evaluated as,

$$q_1 = V_c.\delta \int_0^1 (u/V_c) \, d(y/\delta) \qquad \text{----------(A.8.7)}$$

From the Blausius solution the value of the integrand was evaluated and found to be given by,

$$q_1 = k_1 . V_c . \delta \quad \text{----------(A.8.8)}$$

where,

$$k_1 = .727$$

Similarly from Keulegan's work (11), q_2 can be calculated,

$$q_2 = k_2 . V_c . y_s \quad \text{----------(A.8.9)}$$

where,

$$k_2 = .8$$

Substituting the expressions for q_1 and q_2 in equation A.8.6, we get,

$$V_2 . W . H_2 = V_c (W-2\delta)(H_2 - \delta - y_s) + 2H_2 . k_1 . V_c . \delta + V_c . k_1 . \delta (W-2\delta) + V_c . k_2 . y_s (W-2\delta) \quad \text{--(A.8.10)}$$

After rearranging the terms we get,

$$V_2 . W . H_2 = V_c \left[W . H_2 + (1-k_2)(2\delta - W) y_s + (1-k_1)(2\delta - W - 2H_2) . \delta \right] \quad \text{----------(A.8.11)}$$

For various values of X and x , V_c could be calculated from equation A.8.11.

One legitimate assumption which could be made is that boundary layer starts forming at the entrance of the test channel This would lead to the conclusion that at any plane in the test

channel ,

$$x = X - 2$$

where,

X and x are distances in ft.

Table A 8-1 shows difference in the calculated densimetric Froude number,(F_2),and the existing free stream densimetric Froude number,(F_c),based on the above analysis. The results are plotted in Fig. A 8-2.

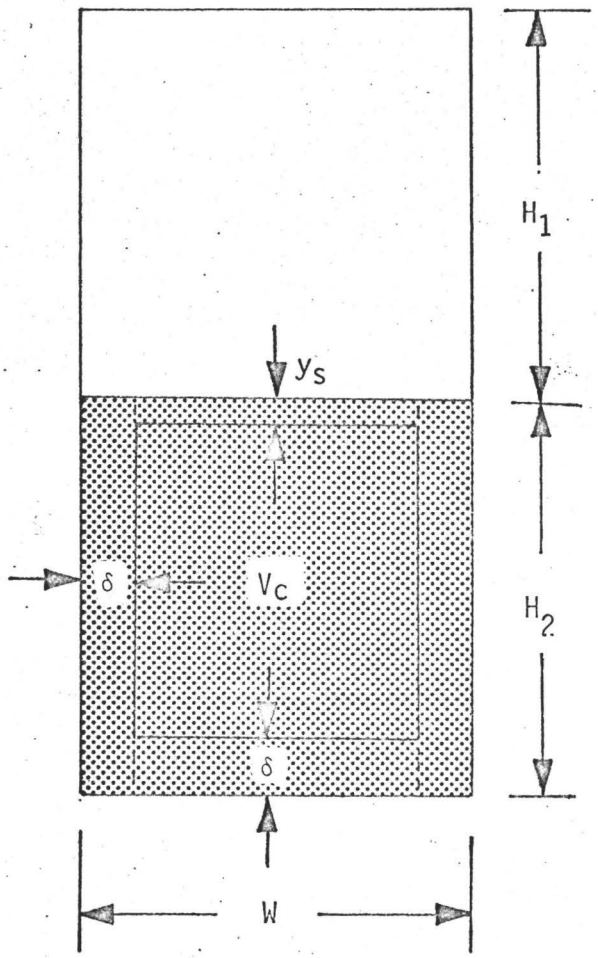

FIGURE A 8-1: BOUNDARY LAYER THICKNESS AT A GIVEN CROSS SECTION.

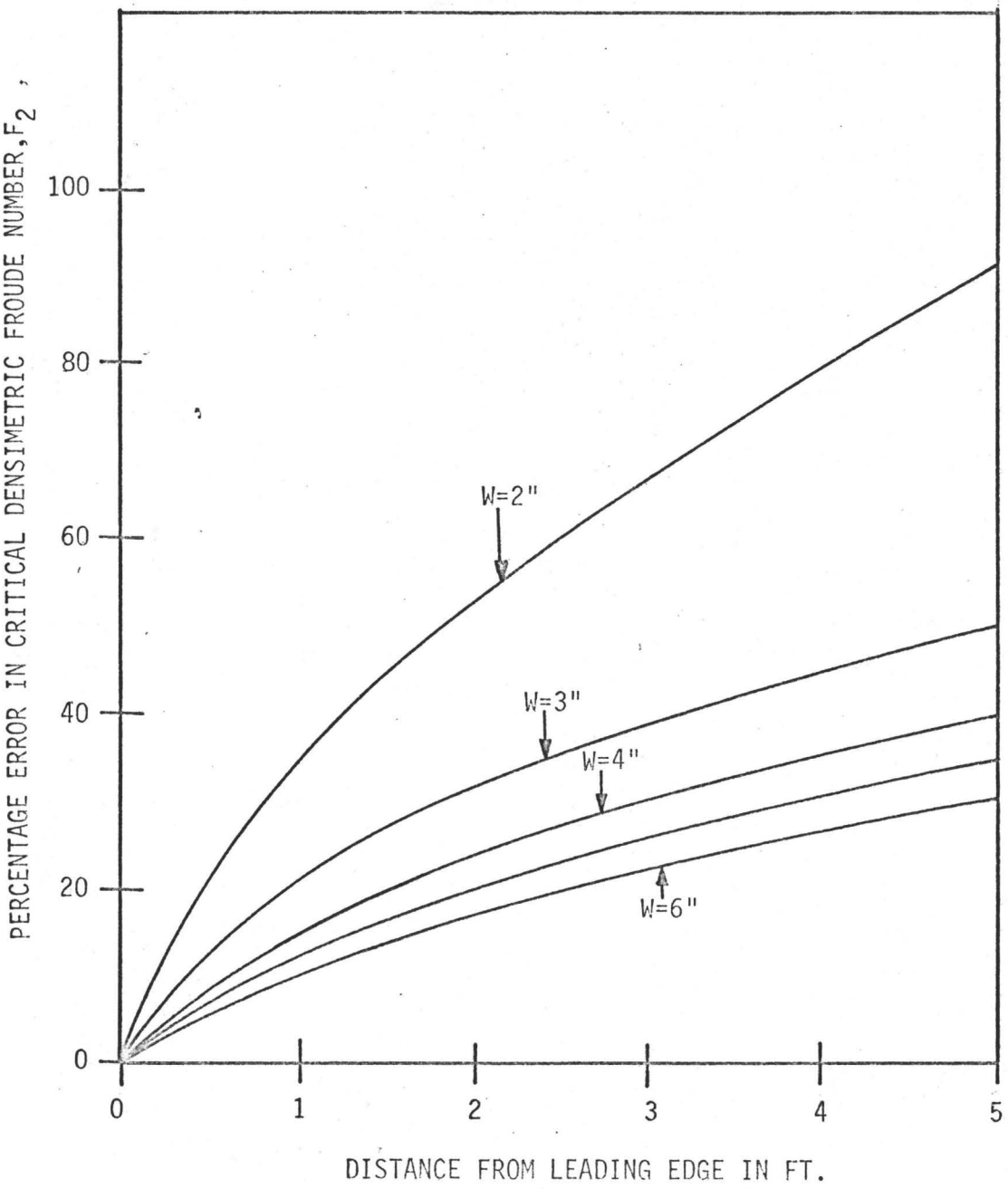

FIGURE A 8-2: PERCENTAGE ERROR IN CRITICAL DENSIMETRIC FROUDE NUMBER, F_2, vs. DISTANCE FROM LEADING EDGE.

TABLE A8- 1

$\Delta S/S_2 = .0200$

NO.	X	W=2"; F_2=.12		W=3"; F_2=.21		W=4"; F_2=.255		W=5"; F_2=.267		W=6"; F_2=.28	
	ft.	F_c	E	F_c	E	F_c	E	F_c	E	F_c	E
1	1	.164	36	.256	22	.295	16	.302	13	.312	11
2	2	.185	54	.276	31	.314	23	.318	19	.327	17
3	3	.202	67	.292	39	.332	30	.336	26	.338	21
4	4	.217	80	.304	45	.344	35	.348	30	.355	27
5	5	.231	92	.316	50	.354	40	.361	35	.364	30

APPENDIX-9

EFFECT OF TEMPERATURE CHANGE

The fresh water coming out of supply tap was below room temperature. This cold fresh water, when issuing over the sugar solution, which was at the room temperature, established a temperature gradient in the two fluids.

This temperature gradient would result in an uncertainty in the specific gravity measurement, thus causing an error in the densimetric Froude number and other measured quantities.

The maximum difference between the temperature of the fresh water and that of the sugar solution and varsol was about 7^{o} F. This would result in an error in the pertinent parameters as follows,

Quantity	Maximum Error Estimated
F_2	.74%
F_H	.37%
Q_2/Q_c	.37%

These uncertainties are sufficiently small and can be neglected for the present work.